THE UNIVERSITY OF ALBERTA

Reversible Generation of Second Sound

By

George Shipley

A THESIS

SUBMITTED TO THE FACULTY OF GRADUATE STUDIES

IN PARTIAL FULFILLMENT OF THE REQUIREMENTS FOR THE DEGREE

OF MASTER OF SCIENCE

DEPARTMENT OF PHYSICS

EDMONTON, ALBERTA

DECEMBER, 1963

1964

TABLE OF CONTENTS

Acknowledgements

Chapter 2 - Temperature Amplitude Determination of Second Sound

Chapter 3 - Experimental Apparatus

Chapter 4 - Electronics

TABLE OF CONTENTS (continued)

Chapter 5 - Experimental Procedure

Chapter 6 - Results

ACKNOWLEDGEMENTS

I would like to thank Dr. F.D. Manchester, my thesis supervisor, for suggesting this project, and for many helpful discussions.

Thanks are due to Messrs. H. McClung, P. Crouse, and J. Legge for help and ideas concerning many technical problems. Mr. J. Rogers provided very welcome help on several occasions, and I would like to thank Mr. H. McCullogh for drawing my attention to the frequency doubler used in this project. I am indebted to the Geophysics and Nuclear Physics Departments for use of a variety of electronic apparatus.

I am grateful for the Assistantship given to me by the University of Alberta, and for the summer grants made available by the National Research Council - without this financial help, this thesis could not have been written.

ABSTRACT

This thesis discusses experiments done on the generation and detection of heat waves in liquid helium. The experiments were carried out in the temperature range from 1.25 to 2.17°K.

The heat waves were detected in the form of standing waves; a thermometer formed one end of a cylindrical cavity, and a heater, consisting of a paramagnetic salt subjected to an alternating magnetic field, formed the other end. The thermometer, in addition to measuring the temperature amplitude of the heat waves, reflected the waves produced by the salt, thus producing standing waves.

The characteristics of these heat waves are well known. The reason for doing the experiments was not to make measurements on the properties of liquid helium, but rather to develop the technical aspects of producing heat waves with a paramagnetic salt so the techniques could be extended to other types of experiments, both on helium, and on solids.

Chapter 1

INTRODUCTION

From its boiling point of 4.21° (Kelvin) down to 2.17°, liquid helium behaves much like any other liquid. At 2.17°, the specific heat shows a lambda transition, and this temperature is referred to as either the transition temperature, or as the lambda point. (A discussion of lambda transitions and related phenomena is given by Pippard (1957), chapter 9; additional references to lambda transitions appear in Squire, (1953), page 210.). From the lambda point down to 0°, helium remains a liquid unless a pressure of approximately 25 atmospheres is applied. This is true for both isotopes of helium, He^3 and He^4. He^4 is the isotope of interest in this thesis, and unless otherwise specified, all references to helium imply He^4. Phenomena that are unique to helium below the lambda point are: a "creeping" film; the thermo-mechanical, or "fountain" effect; an extremely high thermal conductivity; the ability to propagate heat waves (or temperature waves, or entropy waves); and, under certain experimental conditions, a coefficient of viscosity of 10^{-11} poise. For comparison, the

coefficient of viscosity of water is 10^{-5} poise, and that of He gas at low temperatures is 10^{-5} poise. This low viscosity gave rise to the term "superfluid" to describe He_{II}. For brevity, helium above its transition temperature is called He_{I}; below, He_{II}.

Also, right at the lambda point, a number of other quantities indicate the presence of a transition by showing either an anomaly (specific heat, and attenuation of sound), or a discontinuity of slope (velocity of sound, and density).

Tisza, (1940) was the first to predict the existence of temperature waves in He_{II}, and his predictions arose out of a two-fluid model he developed to explain the extraordinarily high heat conductivity that had been observed in He_{II}.

Independently of Tisza, Landau (1941) developed a quantum-hydrodynamical set of equations to describe liquid helium. He obtained two wave equations, and Landau named the phenomena his equations described, first sound and second sound. First sound was the propagation of pressure variations, but he did not specify what property second sound was propagating. In 1944, Lifschitz made the prediction, based on development

of Landau's theory, that second sound should be thermal in nature. The first experimental observations of second sound were made by Peshkov in 1944, and second sound was indeed thermal waves.

Tisza and Landau predicted the same effect; however, their theoretical models were very different.

Tisza based his model on an application of the Bose-Einstein condensation to helium as developed by London (1938). Since the nuclear spin of He^4 is zero, He^4 atoms obey Bose-Einstein statistics; London considered helium to be a gas of non-interacting bosons, and with this model calculated a "degeneracy" temperature of 3.13°. The specific heat showed a discontinuity in slope at the degeneracy temperature, and the shape of this theoretical specific heat curve was similar to the observed specific heat curve (compare the theoretical curve, (London (1954)), page 41, with the experimental graph, (Daunt and Smith, (1954), page 173)). Below this degeneracy temperature, helium atoms begin "condensing"; these atoms are spread uniformly throughout the gas, but they are in the lowest energy state, and all have the same momentum; that is, they are "condensed" in momentum space. The superfluidity of He_{II} was

attributed to these condensed particles.

Refinements to the Bose-Einstein condensation model have brought the theoretical specific heat curve closer to experimental data down to 0.6°, but none of the refinements predict the observed T^3 dependence of the specific heat for $T < 0.6^\circ$.

Tisza, then, developed a macroscopic, two-fluid hydrodynamics in which the superfluid was composed of the condensed bosons, and the normal fluid the uncondensed bosons. In his formulation, Tisza assumed that the superfluid particles, as well as the uncondensed atoms, could sustain Debye excitations. For the temperatures between 1.0° and 2.17°, London and Tisza developed the following semi-empirical equation for the velocity of the temperature waves:

$$u_2 = 26\ (T/T_\lambda \left[1 - (T/T_\lambda)^{5.5}\right])^{1/2}, \text{ meters/sec} \qquad (1)$$

where u_2 is the velocity of the heat waves, T the absolute temperature, and T_λ the observed transition temperature. In addition, Tisza (1947) predicted that as T approached 0, u_2 would approach 0.

A consequence of Tisza's two-fluid model was that, during temperature wave propagation, the super and normal components would oscillate out of phase with each other. This can be seen from the equation for mass flow,

$$\bar{J} = \rho_s \bar{v}_s + \rho_n \bar{v}_n \tag{2}$$

where J = mass/cm^2 -sec and v_s, and v_n, are the velocities of the super and normal components*. When temperature waves are propagated, there is no net mass motion, therefore,

$$\bar{J} = 0$$

and

$$\bar{v}_s = -(\rho_n/\rho_s)\ \bar{v}_n \tag{3}$$

that is, the two components are 180° out of phase. (For density propagations, that is, sound, the two components are in phase)

---

* v_s and v_n are particle velocities, and are on the order of 10 cm/sec when u_2 is 2000 cm/sec. Values for v_n are obtained from $W = \rho\ sTv_n$, where W is the heat input, watts/cm^2. ρ_s/ρ_n is obtained either from equation (4), or from oscillating disk experiments.

Landau's theory had no explicit dependence on the type of statistics the atoms should obey; more important to him was the fact that helium remained a liquid down to 0°. At 0°, the helium was considered to contain no excitations, that is, the liquid was in its ground state.

Above 0°, there were two types of excitations in the helium: the first was phonons; and the second was quantized vortices which Landau called rotons. In this theory, the phonons and rotons were superimposed on the background fluid; the background fluid could support no excitations, and composed the superfluid of He_{II}; the phonons and rotons composed the normal part of He_{II}.

The equation Landau derived for the velocity of second sound was

$$u_2 = \sqrt{\frac{\rho_s \ Ts^2}{\rho_n \ c_v}} \qquad \text{meters/sec.} \qquad (4)$$

where u_2 is the velocity, ρ_s and ρ_n are the densities of the super and normal fluids (and obey the relation $\rho_s + \rho_n = \rho$; ρ is the bulk density of the liquid), s is the entropy in joules/kgm-deg, c_v the specific heat in joules/kgm-deg, and T the absolute temperature.

Landau's calculations based on (4) showed u_2 approached $u_1/\sqrt{3}$ as T approached zero, where u_1 is the velocity of first sound at 0°.

Before stating some of the experimental results, it should be mentioned that the theories of Tisza and Landau developed wave equations, and not diffusion equations, for the propagation of heat. That is the velocity was independent of frequency; and, to first order approximation, there was no attenuation. This is in contrast to ordinary heat conduction, where heat propagation is described by the diffusion equation. The solution to the diffusion equation shows that the velocity of the heat waves (assuming a sinusoidal heat current) is proportional to the square root of the frequency, and the temperature amplitude falls to 1/e of its original value in 1 wavelength; (see Howling, Mendoza, and Zimmerman (1955), or Carslaw and Jaeger (1959), page 64).

The first measurements on second sound were made in 1944, and by 1954, the question of the value of the velocity as T approached zero was settled. de Klerk, Pellam, and Hudson (1954) measured the velocity down to 0.015°, and found agreement

with Landau's theory. (Actually, the measurements showed u_2 equal to $u_1/\sqrt{3}$ at 0.5°, and u_2 seemed to approach u_1 as T went to 0. However, this "overshooting" can be explained, since a) the thermal excitations below 0.6° are mainly phonons, and b) the mean free path of the phonons was longer than the dimensions of the apparatus; therefore, phonons leaving the heater were able to travel to the thermometer without colliding with another phonon. Since phonons travel with velocity u_1, u_1 was observed for the velocity of u_2 as T went to 0.)

Within experimental accuracy, second sound has shown no dispersion in the frequency range from 10 cycles per second (cps), (Peshkov, (1949)), to 600 kc, (Mercereau, Notarys, and Pellam, (1961)). The wave nature of second sound has been demonstrated in a variety of other ways: the most common method of study has been standing wave and pulse techniques, see Peshkov (1960) and references cited therein; the experiment of Mercereau et al centered around a thermal diffraction grating; and the effects of second sound on a Rayleigh disk have been observed, by Pellam, (1955).

In addition to helping settle the validity of the Tisza and Landau theories*, second sound has been used as a "tool" to investigate various properties of He_{II}: the ratio ρ_s/ρ_n is most reliably obtained from accurate measurements of u_2, see equation (4); the attenuation of second sound provides a measure of irreversible processes in He_{II}; when second sound is produced in rotating He_{II}, there is additional attenuation, and measurements of this attenuation have been used to study the mutual friction between the normal and super fluids, (Hall and Vinen, (1956)). Second sound has also been used to gain information about quantized vortex lines in He_{II}, (Bablidze (1963)).

Almost all of the experiments involving second sound have used a resistance heater to produce the temperature fluctuations. A resistance heater produces a d.c. component of heat flow superimposed on the fluctuating heat propagation;

---

* Although developments and extensions of Landau's theory have enjoyed many successes, his model describes only the low-temperature side of the specific heat curve; in addition, it does not exclude the possibility of superfluidity for He^3. While it is possible that He^3 will become superfluid, no transition has been observed down to 0.008°, (Anderson, et al (1961)).

however, the steady flow does not affect any properties of second sound (velocity, attenuation), because a d.c. heat flow can be regarded as second sound of zero frequency.

In the thermodynamic sense, the presence of the d.c. heat flow makes the production of second sound by resistance heaters "irreversible generation". Reversible generation has also been used, the most notable examples being experiments of Peshkov (1948), and Kurti and MacIntosh, (1955).

Peshkov generated first sound in a cylindrical cavity, and at one end of the cavity he had a copper-disk superleak*. Only superfluid could pass through the superleak, and since the temperature of the superfluid is 0°, "cold" waves were generated outside the cavity. The cold waves were of course second sound, but instead of the temperature fluctuations being positive with respect to the bath temperature, as in the case of irreversible

---

* A superleak is a very small opening, approximately 10^{-5} cm, across that allows only the superfluid to pass. Superleaks that have been used by various investigators are: spaces between optical flats; hard-packed jeweler's rouge; and fine wires pressed tightly together, confined in a tube.

generation, the fluctuations were less than the bath temperature.

Kurti and MacIntosh used a paramagnetic salt subjected to an alternating magnetic field, thus producing alternate heating and cooling. They measured the velocity of second sound between 1.3° and the lambda point, and as expected, obtained the same values as investigators who used irreversible heaters.

The experiments described in this thesis parallel those of Kurti and MacIntosh, and some of Peshkov's. The purpose of the experiments was not so much to investigate properties of second sound in greater detail, but rather to develop the technology of reversibly-generated second sound so that it could be used for future experiments.

There has been some discussion as to the possibility of exciting second sound in solids: the two-fluid concept applied to superconductors led Bardeen and Schrieffer (1960), page 266, to discuss second sound in superconductors; however, they discount the possibility because collisions between normal electrons and impurities are much more frequent than electron-electron collisions. Gorter (1955) dismisses second sound in superconductors for essentially the same reason.

However, Ginzburg (1962) revived the issue in an effort to explain the two phenomena encountered with superconducting Pb and Hg; "precursor absorption", and the deviation of the electronic specific heat from the BCS theory. Ward and Wilks (1951) discuss the possibility of second sound in very pure crystals; and Dingle (1952) made calculations for the velocity of second sound in gases, insulators, conductors, superconductors, and ferromagnets. Chester (1963) has shown the possibility of temperature waves existing in dielectric solids; Chester's analysis is based on a modified entropy-conservation heat equation, and, unlike others, does not depend on a super and normal fluid division.

In looking for second sound in solids, the use of a reversible generator would be preferable to a resistance heater; the latter would produce a steady heat flow from the source, and it would be simpler to deal with temperature fluctuations in the absence of this heat flow.

Also, reversibly generated second sound, in conjunction with the analog of a Helmholz resonator, could be used to study the mutual friction existing between the normal and superfluid components, (Manchester (1957)).

Another application of reversible generation might be in very low temperature investigation of second sound. In addition to eliminating joule heating, heat leaks due to the heater wires would be eliminated. However, spin-lattice relaxation times become very long as the temperature is decreased; also, a salt would have to be found that had a Schottky anomaly below the temperature at which one wished to work.

Keeping in mind the requirements of possible future experiments, the problems that had to be solved can be outlined as follows.

A continuous wave, reversible generator of second sound was wanted, and a magnetically driven paramagnetic salt could provide this. To be useful experimentally, the salt had to produce a large enough temperature amplitude to be detected; and it had to have a spin-lattice relaxation time below 2° that was fairly short, otherwise frequencies would have to be used that would produce wavelengths longer than a convenient size of resonator.

Once the working frequencies were thus determined, a means of producing and detecting the temperature fluctuations in the helium had to be obtained. The main problem here was

in detection; a suitable thermometer had to be found, and electronics that were sensitive enough to detect the weak signals generated in the thermometer circuit had to be developed. The electronics detection was simplified somewhat by the fact that the frequency of second sound was twice that of the driving frequency. This was a simplification because it allowed the use of filters; why the frequency was doubled will be explained in the next chapter.

Chapter 2

TEMPERATURE AMPLITUDE DETERMINATION OF SECOND SOUND

Frequency Doubling

In continuous wave generation by both resistance heaters and by a paramagnetic salt, the frequency of temperature variation is twice that of the driving frequency.

For resistance heaters, if the resistance is R, and the current through the resistor is $I_0 \cos \omega t/2$, then the energy/unit time generated in the resistor is

$$RI_0^2 \cos^2(\omega t/2) = 1/2\ RI_0^2 + 1/2\ RI_0^2 \cos \omega t \qquad (5)$$

Thus the "a.c." part of the heat production has an angular frequency of ω.

When a magnetic field is put on a paramagnetic salt, the resultant spin of the paramagnetic ion lines up with the field, thus absorbing energy from the field. This energy is communicated to the lattice in a length of time given by the spin-lattice relaxation time, and in our case, then to the helium, thereby heating the helium. Since the process is

reversible*, when the magnetic field is removed, the spins will become disoriented, absorb energy from the lattice, and cool the helium.

If the field is now reversed, the spins again line up, producing a heating. Diagrammatically, we can see this heating and cooling on an entropy vs. temperature curve of a paramagnetic salt; Figure 1.

From 1 to 2, a magnetic field of magnitude H_1 is applied suddenly, and the temperature increases to T_2. H_1 is left on until the temperature of the salt comes back to T_{bath}. Then the field is reduced to zero, and the temperature drops to T_4. The temperature of the salt will then return to T_{bath}. If the cycle is now repeated, but with H_1 in the opposite direction, the same path on the S vs T diagram will be traced.

If we want to plot the above sequence on an H vs time diagram, we would have the following; Figure 2.

---

* The process is not strictly reversible, due to the non-zero spin-lattice relaxation time. This departure from reversibility is manifested in the lattice temperature amplitude being smaller than the spin amplitude; the effect on the helium temperature amplitude will be taken up later.

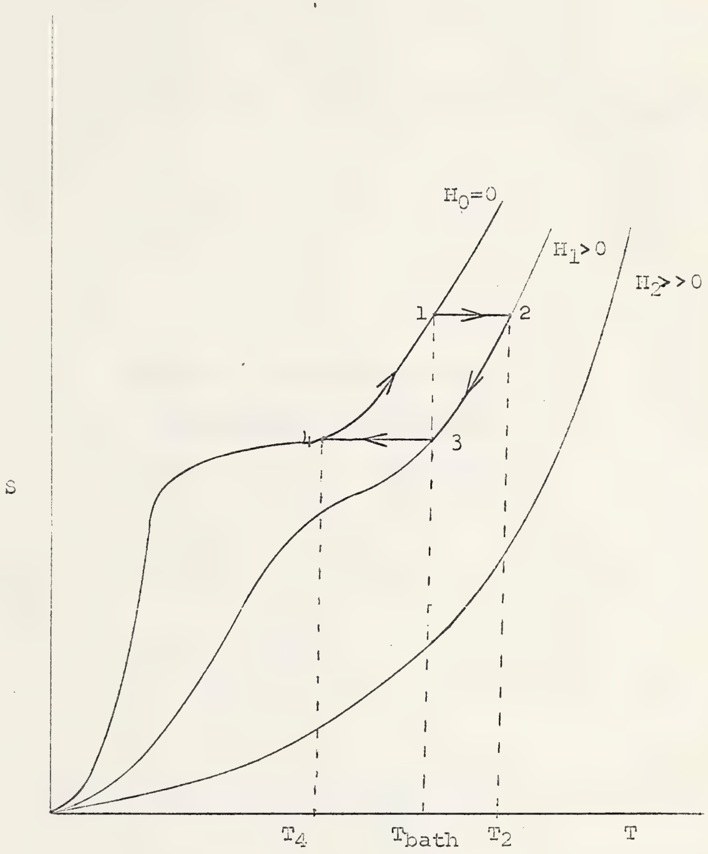

Figure 1 - Entropy vs Temperature Diagram for a Paramagnetic Salt Below 5°K

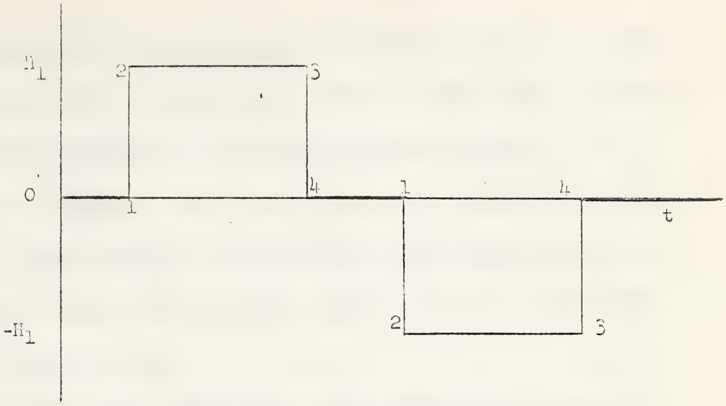

Figure 2 - H vs t for the

Cycle Shown in Figure 1

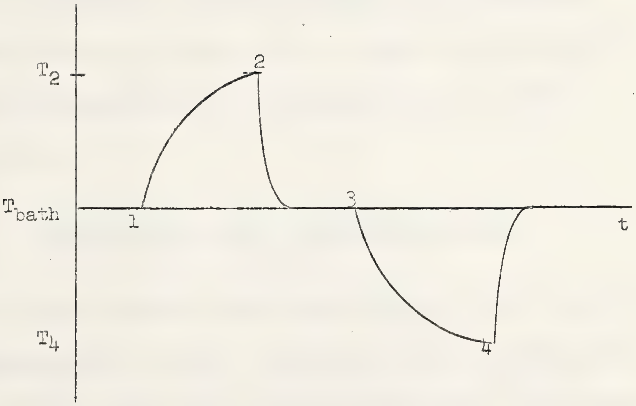

Figure 3 - Helium Temperature vs t Resulting

from Figures 1 and 2

The numbers in Figure 2 correspond to those in Figure 1, and the resulting T vs t curve would actually look like; Figure 3.

If the magnetic field is sinusoidal instead of the square wave of Figure 2, all the corners in Figure 1 would be rounded off, the amount of rounding and distortion depending on the ratio of the period of the magnetic field to the spin lattice relaxation time.

From the above discussion, it is seen why frequency doubling occurs; it is also noticed that with a square wave magnetic field on a paramagnetic salt, information regarding spin-lattice relaxation should be obtainable; also, from Figure 1, it should be possible to obtain the shapes of the families of curves H = constant on the S vs T diagram.

The choice of a salt, with regard to its temperature amplitude and spin-lattice relaxation time, is taken up in the next section.

Calculations for a Paramagnetic Salt

To obtain temperature amplitudes in the helium and in the thermometer for a given magnetic field, the analysis given by Atkins (1959), page 144, will be followed. The temperature

amplitude in the helium will depend on the amount of heat/cm^2-sec flowing into the helium. This heat flow will be governed by 1) the amount of energy made available by the magnetic field, 2) the spin-lattice relaxation time of the salt, 3) the thermal impedance of the salt, 4) the thermal boundary resistance that exists between the salt and the helium, and 5) the thermal impedance of the helium. The temperature amplitude seen by the thermometer will depend on the heat flow in the helium, the thermal boundary resistance between the helium and thermometer, and the thermal impedance of the thermometer.

The energy made available by the magnetic field can be obtained if we first consider the salt to be isolated from the helium; the temperature rise of the salt for a given magnetic field is then calculated, and the energy is the product of this temperature rise and the specific heat of the salt.

Since (at low frequencies) irreversible effects are negligible, the Tds equation of the salt is given by (6),

$$Tds = c_l dT + c_s dT + T(\partial M/\partial T)_H \, dH \qquad (6)$$

where s = entropy/cm^3, c_l and c_s are the specific heats of the lattice and spins ($c_s = (\partial q/\partial T)_H$), M = total magnetic moment, and H is the applied magnetic field - for the Tds equation of a paramagnet, see Zemansky (1957), page 310.

(Changes of pressure have been ignored in (6).) Values for the quantities in (6) are,

$$\left.\begin{aligned} c_1 &= 10^{-5}T^3 \text{ joules/cm}^3\text{-degree} \\ c_s &= 4.8\ 10^{-4}/T^2 \text{ joules/cm}^3\text{-degree} \end{aligned}\right\} \quad (7)$$

de Klerk (1956), page 98. We know that $M = -bH/T$, where b = the Curie constant. Therefore, $T(\partial M/\partial T)_H = -bH/T$. We are considering a thermally isolated salt, therefore, $ds = 0$; also, c_s is approximately 40 times as large as c_1, and thus, c_1 will be neglected. dT from (6) is then given by

$$dT = bHdH/Tc_s \ . \quad (8)$$

The amount of heat generated per unit time and per cm^3 will be $I = c_s dT/dt$. If $H = H_0 \exp i(\omega/2)t$, this gives,

$$I = i(\omega/2)b\, H_0^2 \exp(i\omega t)/T \text{ joules/sec-cm}^3 \quad (9)$$

Before finding the effect of the spin-lattice relaxation time on (9), the two main relaxation effects in paramagnetic salts will be mentioned. There is a spin-spin relaxation time, independent of temperature, which is approximately 10^{-9}sec. This means that as long as the frequency of an applied field is significantly less than 10^9 cps, the spins will all be in thermal equilibrium.

The spin-lattice relaxation time is determined by the time it takes the magnetic spin energy to be communicated to the lattice, and is on the order of 10^{-3} sec at 2°K. The means of energy communication is provided by the thermal motion of the lattice. This motion perturbs the electronic orbits, disrupts the spin-orbit coupling, and thus provides a spin-lattice interaction. Since the lattice vibrations decrease with decreasing temperature, we have a qualitative reason why the relaxation time increases with decreasing temperature*. To find the effect of spin-lattice relaxation on I of (9), we follow the model of Casimir and du Pre (1938), and assume that the rate of heat flow from the spins to the lattice is proportional to the difference in temperature between the spins and lattice. Or,

$$dq/dt = \alpha(T_s - T_l) \tag{10}$$

where T_s is the spin temperature and T_l the lattice temperature; we also know that

$$dq = c_l dT_l \tag{11}$$

---

* For a fuller discussion of paramagnetic relaxation phenomena, see Cooke (1950), or Pake (1962), Chapter 6.

Solving for T_1 from (10) and (11), subject to the condition that $T_1 = T_s$ at $t = 0$, we find

$$T_1 = T_s(1 - \exp(-\alpha/c_1)t) \qquad (12)$$

To continue the analysis, we note that if one had a resistor $1/\alpha$ in series with a capacitor c_1, then for an input voltage of T_s, the voltage across the capacitor would be given by (12); (12) also defines a time constant,

$$\tau = c_1/\alpha \qquad (13)$$

(In Casimir and du Pre's model, spin-lattice energy was considered to flow from the lattice to the spins; the result is that, in the literature, τ is given by $\tau = c_s/\alpha$, and not by c_1/α. However, τ does not depend on which direction the energy flows; therefore, the values of τ quoted in the literature can be used for this analysis.)

If $T_s = T_s \exp(i\omega t)$, then T_1 will be

$$T_1 = T_s \frac{1/i\omega c_1}{1/\alpha + 1/i\omega c_1} \qquad (14)$$

or

$$T_1 = T_s\, e^{-i\theta}/(1 + \omega^2\tau^2)^{1/2} \qquad (15)$$

where τ is given by (13), and the phase factor is $\theta = \omega\tau$. At low frequencies, $T_1 = T_s$; therefore, T_s would be given by (8), and the modified form of (9) will be,

$$I = \frac{1/2\,(\omega b)\ H_0{}^2 e^{i\phi}}{T(1 + \omega^2\tau^2)^{1/2}} \quad \exp(i\omega t), \frac{\text{watts}}{\text{cm}^3} \qquad (16)$$

and $\phi = \pi/2 - \omega\tau$.

All of the heat generated in the salt will not be able to reach the helium. If only the salt, to a depth β, gives heat to the helium, then the heat current available to the helium will be

$$I = \frac{\omega b\ H_0^2\ \beta\ e^{i\phi}}{2T(1 + \omega^2\tau^2)^{1/2}}\ e^{i\omega t} \quad \text{watts/cm}^2 \qquad (17)$$

The next item of interest is the thermal impedance of the salt. For a substance that obeys the thermal diffusion equation, the thermal impedance is given by

$$Z = \left[(1 + i)(\pi fck)^{1/2}\right]^{-1} \text{degree-cm}^2/\text{watt} \qquad (18)$$

where f is the frequency of the temperature fluctuations, c is the specific heat in joules/cm^3 -degree, and k is the thermal conductivity in watts/cm-degree; see Dingle (1948).

For an insulator at low temperatures, the thermal conductivity can be expressed by $k = 1.6 \times 10^3 A^{2/3} d\ T^3$ watts/cm-deg, where $A = c_1/T^3$, and d is the average distance between grain boundaries; see White (1959), page 245. For powdered iron alum, the upper limit of d will be the granule size, approximately 10^{-2} cm; the maximum value of k is then $k = 8 \times 10^{-3} T^3$ watts per cm-degree. Using c_s in (17) and neglecting the phase factor, Z becomes

$$Z \simeq 10^3\ (fT)^{-1/2}\ \text{deg-cm}^2/\text{watt}. \tag{19}$$

The thermal boundary resistance, or "Kapitza resistance", between the salt and helium is approximately $40\ T^{-2.6}$ deg-cm^2 per watt*; and will be assumed to be resistive only.

The Kapitza resistance is characterised by a temperature discontinuity between two materials in physical contact. Kapitza was the first to notice it; he noticed it between a copper block and He_{II}. The discontinuity has also

---

* This value was taken from White et al (1953); the Kapitza resistance has not been measured for a paramagnetic salt, but the values obtained for different materials are the same within a factor of 10.

been observed in He_{II} and He^3. Current theories dealing with the cause of the Kapitza resistance do not agree very well with experiments; (Toronto Conference (1961), Chapter 20), and (Little (1963)).

Since heat flow in He_{II} obeys a wave equation and not the diffusion equation, the thermal impedance of He_{II} cannot be determined in the same way as was done for the salt. The propagation of temperature disturbances in He_{II} is similar to the propagation of voltage disturbances in a transmission line. Actually, second sound waves are more similar to ordinary sound waves than to electromagnetic waves. Behaviour of particle motions in first and second sounds are similar; and boundary conditions, for example, in a resonator, are much the same. The result is that (for resonators) temperature distributions are the same as for pressure distributions in first sound, and many of the electromagnetic modes do not appear. However, some electromagnetic analogs are appropriate to second sound propagation, and one of these, the impedance analog, is made use of below.

By noting that temperature fluctuations correspond to voltage, and heat current corresponds to electric current, the "characteristic" thermal impedance of He_{II} is found to be

$$\gamma = \frac{1}{\rho c u_2} \; \frac{\text{cm}^2\text{-deg}}{\text{watt}} \tag{20}$$

Osborne (1948), (1951), and Dingle (1948).

We are now in a position to set up the heat flow equations. Denoting the Kapitza resistance by R, the paramagnetic salt by the subscript "p", the helium by "H", the amount of heat/cm^2-sec. flowing into the salt-helium system by I, (equation (16)) and understanding a time variation on all expressions to be exp(iωt), we have,

$$I = I_p + I_H, \tag{21}$$

$$I_H = (T_p - T_H)/R, \tag{22}$$

$$I_H = T_H/\gamma\ , \tag{23}$$

and

$$I_p = T_p/Z. \tag{24}$$

Using (21) - (24), and solving for T_H gives,

$$T_H = I\left[1/\gamma\ (1 + R/Z) + 1/Z\right]^{-1} \tag{25}$$

In the temperature range 1.2 to 1.4°, $\gamma = 0.03T^{-4.6}$cm^2-deg/watt, Osborne (1948). The minimum value of Z would be at the highest frequencies used, approximately 1000 cps; this makes $Z \simeq 3$ deg.-cm^2/watt; R = 40 deg.-cm^2/watt; the 1/Z in the

denominator in (25) can be neglected, and

$$T_H \simeq A \gamma I \text{ deg.} \tag{26}$$

where A will depend on the frequency, and is less than 1.

We now have an expression for the temperature amplitude in the helium*; to obtain the amplitude in the thermometer, the thermal impedance of the thermometer is needed. The thermometer material was mainly graphite; for pure graphite, $c \simeq 6T \times 10^{-5}$ joules/mole-deg., Keesom and Pearlman (1955), $\rho = 1.6$ gm/cm (measured at room temperature), and $k = 4 \times 10^{-5} T^2$ watts/cm-deg., Berman (1952). For the thermometer, Z becomes

$$Z \simeq 7 \times 10^{-4}/(fT^3)^{1/2} \ \frac{\text{cm}^2\text{-deg.}}{\text{watt}} \tag{27}$$

An analysis similar to the one leading to (26) results in the following expression for T_t, the temperature in the thermometer

$$T_t = T_H Z_t/(Z_t + R); \tag{28}$$

so, $T_t \simeq T_H$. The presence of the thermometer backing has

---

* The derivation of the temperature amplitude in the helium, based on a different approach is given in Appendix 2.

been neglected. The heat flow into the backing could be taken into account, but the thermal conductivity and specific heat of phenolite (the backing material) are not known.

If we take the value of A, equation (26) to be 2/3, the temperature amplitude, between 1.2 and 1.4°, is

$$T \simeq \frac{\omega b\ H_0^{\ 2}\ \beta \times 10^{-9}}{T^{5.6}(1 + \omega^2 \tau^2)^{1/2}}\ \text{deg.} \tag{29}$$

The analysis leading to (29) would apply to a freely travelling wave; the temperature amplitude in a resonator will be greater than that given in (29). The amount of increase would be very difficult to predict. Rayleigh (1896), page 212, and Wood (1930), page 191, discuss the increase in amplitude for sound resonators; the increase is very sensitive to the geometry of the system, and would probably also depend on the thermal properties of the transmitter, receiver, and resonator.

The increase can be measured experimentally. Peshkov (1948) made the approximation that

$$T_H = I/\rho c u_2; \tag{30}$$

Peshkov used a resistance heater, so $I = I_0^{\ 2}\ R/2A$, where A was the cross section area of the resonator, R the resistance

of the heater, and I_0 the current amplitude in the heater. At 1.63°, his experimental temperature amplitudes were approximately 10 times greater than predicted by (30).

Choice of Salt

For a given temperature, frequency, and magnetic field, the temperature amplitude in the helium will be determined by the quantity, $b/(1 + \omega^2\tau^2)^{1/2}$; cf (29). For large signals, a salt with large b and small τ was wanted. Table I lists b and τ for some of the common salts in use in low temperature work. The values of b have been taken from Mendoza (1961), page 198; his values of susceptibility have been multiplied by the density of the crystal to give b the proper dimensions for use in (29). Values of τ are from Benzie and Cooke (1950), and are estimates for what τ would be at 1.3°.

Salt	b	τ-sec.
Manganous Ammonium Sulphate	2×10^{-2}	25×10^{-3}
Gadolinium Sulphate	3.3×10^{-2}	25×10^{-3}
Copper Sulphate	3.7×10^{-2}	10^{-5}
Iron Ammonium Alum	1.5×10^{-2}	10^{-3}

Table 1

The salt used in my experiments was iron ammonium alum; due to lack of time, others were not tried. However, since gadolinium sulphate and copper sulphate have practically the same value of b, but values of τ that differ by 2500, they could be used to check the validity of (29). The temperature amplitude of gadolinium sulphate should be independent of frequency above 100 cps, while the temperature amplitude of copper sulphate should increase linearly with frequency up to 10 kc.

Observed Temperature Amplitude

The thermometer used in these experiments was an Allen Bradley radio resistor; a fuller discussion of this thermometer

and a brief mention of other second sound thermometers is given in Chapt.3. These resistors are very temperature sensitive below 4°, i.e. dR/dT is very large. Therefore, when a d.c. current, I, was passed through the thermometer, and its temperature changed by $\Delta T\cos\omega t$, the resulting voltage change,

$$\Delta V = I \Delta R = I \, dR/dT \, \Delta T\cos\omega t \tag{31}$$

was large enough to be measured even when ΔT was only 10^{-6}°.

Now I is measured, dR/dT is determined prior to making second sound measurements, and ΔV is measured with the appropriate electronics; therefore, ΔT is obtained from

$$\Delta T = \Delta V/(I dR/dT). \tag{32}$$

Magneto Resistance

A complication in determining ΔT arose in these experiments, and was due to the fact that the resistance changed under the influence of a magnetic field. Therefore, when the thermometer was down close to the Pb solenoid, the amplifier observed resistance changes induced not only by second sound, but also by the magnetic field.

This magneto-resistance appears to be common to all low temperature resistance thermometers; quantitative des-

criptions of the magneto-resistance of thin-film carbon thermometers are given by Hornung and Lyon (1961); magneto-resistance of Allen Bradley thermometers was investigated by Clement and Quinnell (1952), and they found that the change in resistance was proportional to H^2. This quadratic dependence on H implies that if an alternating magnetic field of frequency f is applied, the resistance should increase twice for every cycle of magnetic field. That is, even in the absence of second sound, the resistance of the thermometer should vary with a frequency of 2f; this was observed to be the case.

So, in order to get an accurate determination of temperature amplitude, the size of the magneto-resistance had to be known. Or, ΔR is no longer given by $\Delta R = \Delta T dR/dT$, but by (neglecting phase factors),

$$\Delta R = (\partial R/\partial H)_T \Delta H + (\partial R/\partial T)_H \Delta T, \tag{33}$$

resulting in a voltage signal given by

$$\Delta V = I\ (\partial R/\partial H)_T \Delta H + (\partial R/\partial T)_H \Delta T. \tag{34}$$

So, to deduce ΔT, we must know $\partial R/\partial H$. (The variation of H with thermometer position must also be known, but this is easily determined.)

To obtain $\partial R/\partial H$, three attempts were made. The first was with a small, static field (a few hundred gauss),

the second with a high, static field (up to 14 Kgauss), and the third with a small, a.c. field. In the d.c. measurements, a chopper amplifier was used to measure resistance changes, Dauphinee and Woods (1955), and the second sound apparatus was used for the a.c. measurements. The results are given in Chapter 6.

Chapter 3

EXPERIMENTAL APPARATUS

Cryostat

A photograph of the cryostat is shown, without the helium and liquid air dewars, in Figure 4. A more detailed photograph of the resonant cavity and thermometer is shown in Figure 5, and a labelled cross section of the cryostat is shown in Figure 6. In Figure 6, region 1 is the experimental chamber, and was usually filled with liquid helium as indicated. The small-diameter tube extending into 1,measured the vapour pressure of the helium; the other end of this tube led to mercury and oil manometers.

The helium bath temperature was controlled by pumping on it, and the bath was pumped on through the large-diameter tube that extends down into 1. This tube went to a mechanical pump, and the pumping rate was controlled by a valve in the line. The rod that supported the thermometer passed down through this pumping tube; also, 1 was filled by first filling 3 with helium, and opening the needle valve. The liquid helium then ran down through this tube into 1.

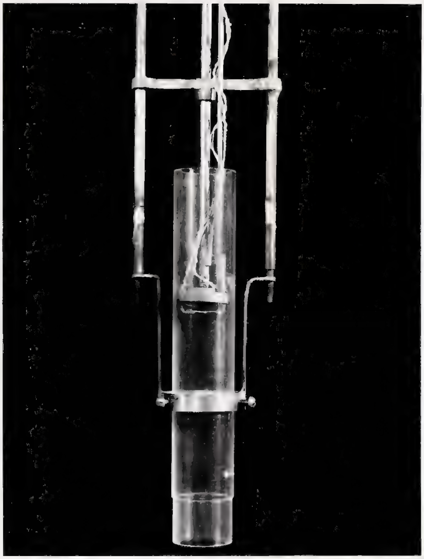

Figure 5 - Resonant Cavity

Figure 4

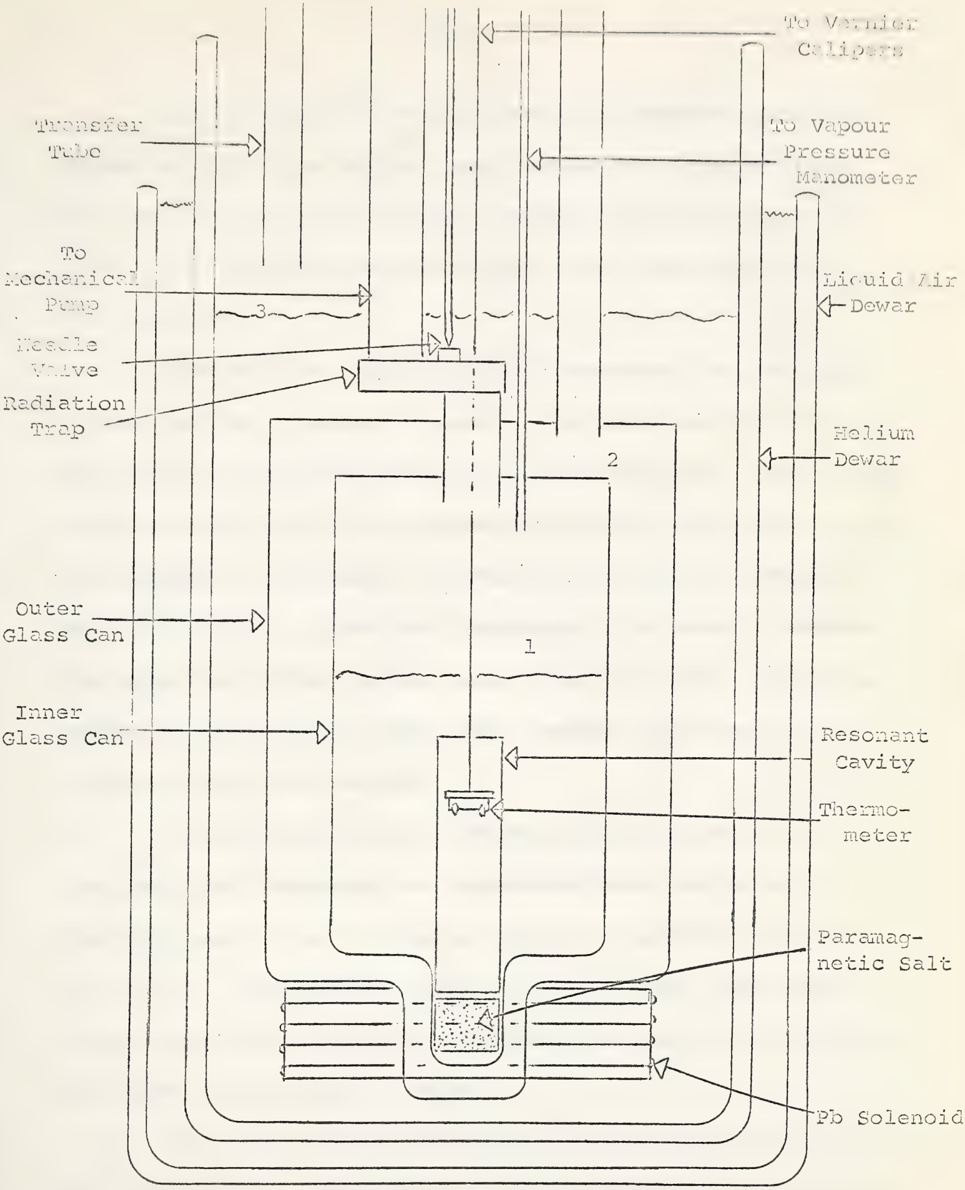

Figure 6 - Cross Section of Cryostat

In an effort to obtain lower bath temperature, 3 was pumped on with a mechanical pump through the transfer tube. This met with limited success; lowering the temperature of 3 from 4.2 to 2.3°K, lowered the inner bath temperature from 1.45 to 1.40°.

The rod that supported the thermometer was attached to one part of a vernier calipers; the other part of the calipers was attached to the top of the cryostat. The rod was moved manually, and the thermometer position read directly off the calipers. An attempt was made to have the thermometer motor-driven by a fractional horsepower d.c. motor. However, the amplifier picked up the noise from the brushes, and this pickup voltage was so great, that despite shielding efforts, the motor could not be used.

A phenolite disk was screwed to the bottom of the rod, and the thermometer was suspended from this backing. The disk was 1.5 cm in diameter, and the resonant cavity was 1.6 cm I.D. The resonant cavity was 12 cm long, and made of lucite; the "thimble" that held the paramagnetic salt immediately below it was also of lucite.

Separate voltage and current terminals were used on the thermometer. The 4 wires to the thermometer were of cop-

per, and 0.003" in diameter; they were unshielded. The voltage leads were twisted together, as were the current leads; with this arrangement, the area of the thermometer was responsible for almost all of the induction pickup.

When the resistance heater was used, the manganin mesh that formed the heater was woven on a phenolite plug, and inserted in place of the paramagnetic salt. Current leads for the heater were brought into this inner chamber through a glass-Kovar "cow" soldered in the top of the inner chamber.

About 3 feet of 0.002" diameter manganin wire was woven into a square mesh, having a resistance of approximately 120 ohms; the thermal inertia of this heater was small enough so that at driving frequencies up to 700 cps, there was no decrease in temperature amplitude for a constant current input. (For frequencies of more than a few kilocycles, however, a drop-off in temperature amplitude could be expected, see Peshkov (1948).)

The alternating magnetic field to which the paramagnetic salt was subjected was produced by a Pb solenoid immersed in liquid helium. Since Pb has a superconducting transition temperature of 7.2°, there was no resistance in the coil, and therefore, no heating.

Pb that was originally 99.999% pure was extruded in the lab into 0.022" wire, and then insulated with a polyurethane coating less than 0.001" thick.

800 feet, comprising 12 layers of 85 turns/layer, were wound on a wooden coil form. The resulting field in the center of the solenoid was found to be 242 gauss (peak one side) per amp (r.m.s.). This calibration was done with a search coil and oscilloscope; details of the search coil are given in Appendix II.

Thermometers

The only feasible method for second sound detection is resistance thermometry. (A number of problems involved in second sound thermometers are mentioned by Snyder (1961); and resistance thermometry for general low temperature applications is discussed by White (1959), chapter 4; Barber (1960); and Hudson (1961).) There are at least five different types of resistors that have been used for second sound detection, and these are listed in Table II. For use as a second sound detector, a thermometer has to have a thermal response time fast enough for the frequencies involved, and it has to

Type	dR/dT	R-ohms	T$^{\circ}$K	References and Comments
Phosphor Bronze Wires	20	10	2.1	Manchester (1957). Phosphor-bronze has been used in pulse methods, Atkins and Hart (1954) and in resonant techniques Peshkov (1960), Hall and Vinen (1956). For details of the wire itself, see Mikhailov and Govor (1962).
	20	4	1.4	
	1	20	2	Barber (1960, page 152.
Allen Bradley Radio Resistor	400	250	1.25	This thesis. Resistance at room temperature, before grinding = 2.7; after grinding = 12.
	$5x10^4$	5000	1.2	Clement et al (1953) - Resistance at room temperature = 10.
IRC Resistance Card	26	200	1.3	This thesis.
	240	2000	1.5	Fairbank and Lane, (1947). Pellam probably used this type in all his experiments, including the one with f = 600kc. He mentions it explicitly only in one article, Pellam (1949).
Aquadag	34	240	1.5	Hassan (1961)

Table II

Table II (continued)

Type	dR/dT	R-ohms	$T^{\circ}K$	References and Comments
Semi-conductor	2500	4000	1.5	Data from Minneapolis Honeywell; see also Snyder (1962), and Kunzler et al (1957).
	10000	10000	1.5	
Super-conductor	200	?	?	Value of 200ohm/deg. given by Bloor (1960), page 235; Snyder (1962) discusses using the superconducting transition as a thermometer, and says it has been used at frequencies up to 1 Mc. However, the reference he mentions does not discuss this thermometer.
Cu-Pb films	3000	120		Golovashkin and Motulevich (1962) - evaporated thin films of Cu and Pb. dR/dT is constant over the useful temperature range, but this range is only 0.3° at most. They are difficult to prepare and have a short life, but should have extremely good frequency response. In addition, a high measuring current (a few milliamps) can be used.

Table II

have a high enough sensitivity for the temperature fluctuations encountered. In addition, large resistances experience large induction pickup voltages. Therefore, a thermometer for this experiment was wanted that had a response time of one millisecond or less, a high sensitivity, and a low value of resistance -- the last two requirements could be combined by saying a large value of $(1/R)\,dR/dT$ was wanted. (The performance of a thermometer is most often described in the literature by stating the value of $(1/R)\,dR/dT$. However, for the present experiments, it is more meaningful to state the values of both R and dR/dT.)

The thermal response time of a thermometer can be determined if its thermal skin depth is known, and the skin depth is defined in the solution to the heat diffusion equation. The diffusion equation is

$$\partial T/\partial t = D\,\nabla^2 T \tag{34}$$

where $D = k/\rho c$, k being the thermal conductivity in watts/cm-deg., ρ the density in mole/cm^3, and c the specific heat in joule/mole-deg. If the temperature at the surface of an infinitely thick material is given by $T = T_0 e^{i\omega t}$, then the temperature at a depth x will be

$$T(x,t) = T_0 \exp\left[-kx + i(\omega t - kx)\right] \qquad (35)$$

where $k = 2\pi/\lambda = (\pi f/D)^{1/2}$, (Howling et al (1955), or Carslaw and Jaeger, (1959), page 64).

We see that the temperature has dropped to 1/e in a distance equal to $\lambda/2\pi$, the "skin depth". Also, at a depth x, the temperature fluctuations are out of phase with the surface fluctuations by an amount $(\pi f/D)^{1/2}x$.

As can be seen in Table 3, phosphor bronze wires and the IRC resistance card do not have very high sensitivity. However, they have very fast response times, and appear to be the only type of thermometer used in pulsed, and very high frequency second sound. Snyder states that phosphor bronze thermometers can be made thin enough so that 1/k does not approach the diameter until the frequency is greater than 100kc; Mercereau et al (1961) have used resistance strips, probably IRC cards, at frequencies up to 600 kc. Phosphor bronze wire and IRC cards have also been used in resonators working at audio frequencies. For work in resonators, these thermometers present a good "geometry", i.e., they can form one (flat) end of a resonant cavity. An IRC card was tried in one of the present experiments using a paramagnetic salt, and no resonances were

observed. However, the trouble may have been due to difficulties with the electronics.

Since Aquadag is applied as a viscous paste, it is useful when special-geometry thermometers are required, e.g., Snyder (1962). However, its sensitivity is no greater than that of the IRC card.

For the sensitivity requirement, it is seen that an Allen-Bradley radio resistor, a semiconductor, or a superconducting film would be the best. However, R is greater for the semiconductors than for the Allen Bradley resistors; and the super conducting film would be hard to prepare and would have a useful range of only a few tenths of a degree. Also, since Allen-Bradley resistors are inexpensive and readily available, we tried to ensure a fast enough response time for our needs by cutting a 1/2-watt resistor down to a thin slice.

The first attempt at cutting down the resistor was with a milling machine. However, the extreme abrasiveness of the carbon dulled the cutting tool almost immediately, and the resistor always broke before one cut was completed.

Then a small, high speed grindstone was tried and was found to work very well. The central portion of the resistor

was ground down, and a fairly uniform thickness of 0.010" was easily obtained in a matter of minutes; but since resistors less than 0.015" thick were very fragile, most of the thermometers were between 0.015 and 0.020", or approximately 0.040 cm, thick.

Now, the skin depth can be calculated if we assume the material in the resistors has the same thermal conductivity and specific heat as graphite. For graphite, when $T = 2°K$, $c = 3T(1 + T^2)\ 10^{-5}$ joules/mole-deg.; Keesom and Pearlman (1955), $k = 4T^2 \times 10^{-5}$ watts/cm-deg. Berman (1952) $\rho = 1.7\ gm/cm^3 = 0.14\ mole/cm^3$, measured at room temperature. The value of D is

$$D = 200T/(1+T^2)\ cm^2/sec.,$$

and

$$1/k = (D/\pi f)^{1/2} = 5.3\ (T/f)^{1/2}\ cm. \qquad (36)$$

This predicts that the skin depth will equal 0.04 cm at a frequency of 26,000 cps. The highest second sound frequency that was used in these experiments was 1400 cps, and as expected, no attenuation was observed.

Therefore, this thermometer had sufficient sensitivity and a fast enough response time; however, it had the disadvan-

tage of protruding out beyond the backing into the resonant cavity, thus destroying the idealness of the resonator; also, a bit more care had to be exercised in mounting the ground-down resistor than in mounting the IRC card.

Resonant Cavity

The resonant cavity was made of lucite; it was 14 cm long, and 1.6 cm I.D. The temperature distribution in the cylinder can be obtained by using the analysis for first sound, and substituting temperature fluctuations for pressure fluctuations. The following discussion follows the analysis given by Morse (1948), page 398. Using cylindrical co-ordinates, let us take the z origin to be at the salt, the azimuthal angle as ϕ, and the radial position as r. Then, if attenuation is neglected, the temperature distribution is given by

$$T = T_0 \begin{matrix}\cos\\ \sin\end{matrix} m\phi \cos(\omega_z Z/u_2) J_m(\omega_r r/u_2) \exp(-i\omega t) \qquad (37)$$

where

$$\omega = (\omega_r{}^2 + \omega_z{}^2)^{1/2}, \qquad (38)$$

and J_m denotes the m-th Bessel function; the maximum value of r is R, the radius of the cylinder.

First, m in (37) is zero. This is because of the angular symmetry of the generator; and, even if the generator were not angularly symmetrical, the frequencies of the modes with $m \neq 0$ are higher than the frequencies used in these experiments. Therefore, we will be concerned only with J_0.

To determine at what positions longitudinal resonances occur, consider only the longitudinal modes excited. Then for a generating (angular) frequency ω, a temperature antinode will be experienced when

$$\cos(\omega Z/u_2) = \pm 1$$

or,

$$Z = (u_2/\omega) n\pi = \lambda n/2\pi \; ; \; n = 0, \pm 1, \pm 2, \ldots \qquad (39)$$

So, for a longitudinal resonance,

$$\omega_z = n(2\pi u_2/\lambda).$$

For radial resonances, the temperature fluctuations at the wall must be a maximum; therefore, we set the derivative of J_0 equal to zero. First, to be able to use a table of Morse's, we let $\omega_r R/u_2 = \pi\alpha$. Now ω_r can be obtained from the solutions to $(d/d\alpha) J_0(\pi\alpha) = 0$. The roots of the solutions are designated by α_{on}, and are given in Morse,

Table 5, page 399. We have,

$$\pi \alpha_{on} = \omega_r R/u_2.$$

Therefore,

$$\omega_r = \pi \alpha_{on} u_2/R. \tag{40}$$

The particle motion in radial modes is oscillation on a radius of the cylinder; it would be difficult to find first sound transducers to excite and detect radial modes of first sound directly, but a transducer for second sound would be simply a resistance wire strung along the axis of the cylinder. The thermometer could consist of Aquadag painted on the inside of the cylinder. Or, the opposite could be done -- deposit a heater on the inside wall, and use a phosphor-bronze wire strung down the center of the cavity as a thermometer.

In radial mode excitation, if the center wire were of small diameter, there would be a very high heat current density (joules/sec.-cm^2) at the center of the cavity. This radial type of excitation and detection might be an effective way of studying large amplitude second sound. Effects of large amplitude second sound has been studied with pulse techniques by Dessler and Fairbank (1956); and anomalous dependence of resulting temperature amplitude vs heater power was

noted by Peshkov, using continuous wave generation (see Figure 20 of this thesis); a linear increase of attenuation as a function of heater power has been noted by Zinov'eva; and Osborne (1951) has demonstrated shock-wave effects with large-amplitude pulses of second sound.

Also, a direct verification of (37) could be observed by the proper placing of a circular thermometer of the correct radius. To see this, we note that there will be a temperature node at a radius of 0.637 R cm, where R is the radius of the tube*. Therefore, if a thermometer of radius 0.637 R cm were placed at one end of the cavity, it would respond only to longitudinal modes, and its frequency would, in general,

---

* If we consider the excitation of the radial modes only, the temperature distribution will be given by (substitute (40) in (37))

$$T = T_0 J_0 (\pi \alpha_{on} r/R) \exp(-i\omega t) \qquad (41)$$

The first zero of (41) occurs when $\pi \alpha_{on} r/R = 2.405$, Jahnke and Emde (1945). This requires that n = 1. The value of r is then $r = 2.405R/\pi \alpha_{01} = 0.637R$.

be different from the frequencies seen by the radial-mode thermometers. (The frequency fed into the heater would be ω cf (38)).

In the experiments described in this thesis, radial modes might have been excited once or twice: the radius of the cylinder was 0.8 cm, and the helium bath temperatures were such that the velocity of second sound was never less than 1800 cm/sec. The minimum frequency for radial modes is given by

$$f = \alpha_{01} u_2 / 2R = 1380 \text{ cps};$$

the highest frequency employed was 1400 cps. Since $J_0(0) = 1$, the temperature distribution usually was given by

$$T = T_0 \cos(\omega_z Z/u_2) \exp(-i\omega t). \qquad (42)$$

Chapter 4

ELECTRONICS

General Description

A block diagram is shown in Figure 7; the frequencies are shown at each stage, f being the driving frequency. The Pb solenoid was in the outer helium bath, and the thermometer was in the experimental chamber; everything else was located outside the cryostat.

As will be shown in the following section, the function of the bottom half of the circuit was to filter out signals developed in the thermometer circuit of frequencies other than 2f. (These background signals were of frequency 60, 120, 180, and f cps; the harmonics of 60 cycles were generated by various items of power equipment in the laboratory, and f was produced by the Pb solenoid).

The oscillator was a Heathkit Audio Oscillator; supplying the current for the Pb coil was a 60 watt MacIntosh power amplifier, and the ammeter reading the solenoid current was an AVO multimeter.

The thermometer current supply, represented by $I_{d.c.}$

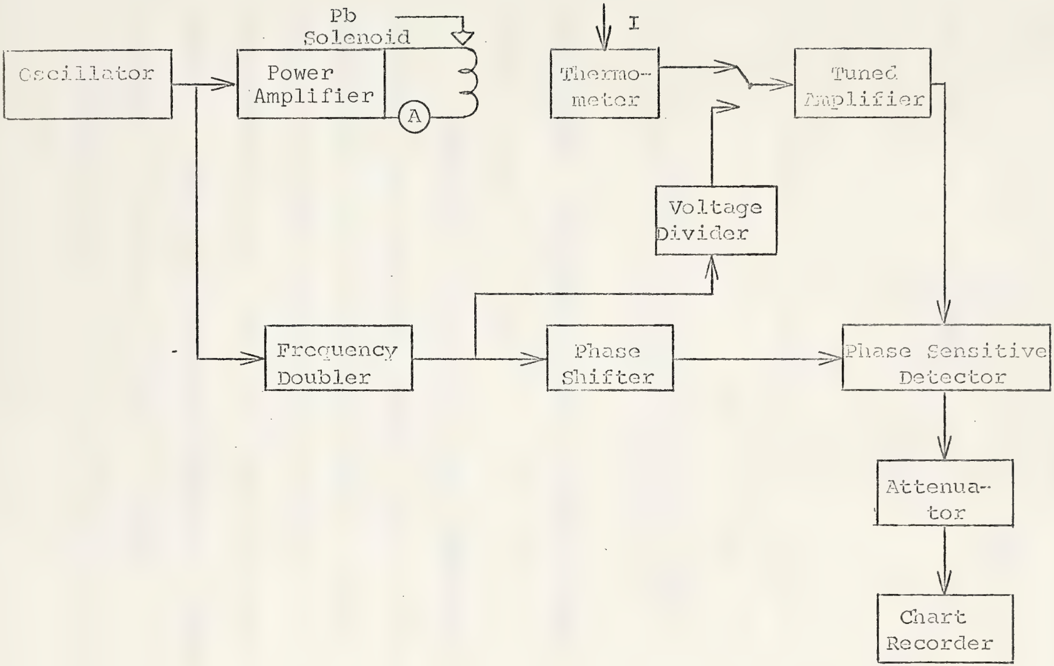

Figure 7 - Block Diagram of Electronics

in Figure 7, consisted of the following; Figure 8

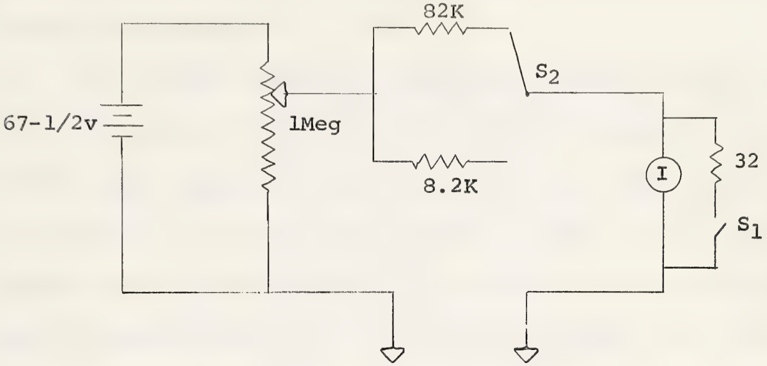

Figure 8 - All Resistances are in Ohms

With S_1 open, the ammeter read 0 to 500 microamps; with S_1 closed, it read 0 to 5 ma.

Amplifying the signals in the thermometer was a General Radio tuned amplifier, Number 1232-A; the output of the amplifier was fed to the signal input of a phase sensitive detector (hereafter called PSD), producing a d.c. voltage of approximately 1 volt. This d.c. signal was fed to a chart recorder, a Leeds and Northrup, Speedomax G. However, this was too large a voltage for the chart recorder, so an attenuator was interposed between the PSD and the chart recorder. The

input of the attenuator was 10 Meg (ohm) resistor in series with a 25k (ohm) rheostat; and the input of the chart recorder looked at the rheostat.

The voltage divider between the frequency doubler and the tuned amplifier was used for calibration purposes. After second sound signals had been observed on the chart recorder with switch S in the position shown in Figure 7, the voltage divider was switched in and adjusted to give an equal deflection on the chart recorder. Voltage V_1 was read with a VTVM, and as the voltage divider had been calibrated beforehand, the voltage developed in the thermometer was obtained without worrying about the gain of the tuned amplifier or the chart recorder, or about the setting of the attenuator.

In this manner the voltage in the thermometer was determined; if we call this thermometer voltage ΔV, then the temperature amplitude is determined by

$$\Delta T = \frac{\Delta V}{I\,(dR/dT)} \quad . \tag{43}$$

Because the second sound signals were often swamped by unwanted signals, the filtering action of the tuned amplifier

was not sufficient; that is, the output of the amplifier, when viewed with a scope, could seldom be positively identified as second sound signals. The additional filtering was accomplished with a phase sensitive detector.

The PSD is discussed in detail in a following section. For the time being, it can be described as follows. If a reference voltage, $V_r\cos(\omega t)$, is fed in to one part of the circuit, and a voltage, $V_s\cos(\omega' t + \epsilon)$ is fed into another part, then the dc output voltage will be proportional to $V_s\cos\epsilon\, \delta_{\omega\omega'}$, where $\delta_{\omega\omega'}$ is the Kronecker delta. That is, there will be a dc response only if the two frequencies are equal, and then the response will be proportional to $V_s\cos\epsilon$.

Since the driving frequency is f, and the second sound frequency is 2f, a voltage source of frequency 2f is needed to act as the reference voltage for the PSD. Also, phase differences will occur not only at various stages of amplification, but also when there are stray inductances and capacitances; therefore, the phase shifter was necessary.

The Pb solenoid is described on page 40; the rest of the apparatus shown in Figure 7 will be described in the following sections.

Tuned Amplifier

A tuned amplifier was built in conjunction with this thesis; it employed a "twin-T" tuning network in a negative feedback arrangement. However, satisfactory results were not obtained, and the GR (General Radio) tuned amplifier was bought. Since a twin-T amplifier described in the literature had better characteristics than the commercial model, and since the principles of operation of the commercial amplifier are similar to the twin-T amplifier, the twin-T amplifier will be described. The twin-T element is shown in Figure 9; it will have a null condition (that is $E_{out}/E_{in} = 0$) for a particular frequency and a particular set of values of its component capacitors and resistors. The conditions for null, Terman and Pettit (1952), page 84*, are

$$C_1 = C_2 = 1/2\ C_3;\ R_1 = R_2 = 2R_3;\ f = \frac{1}{2\pi R_1 C_1} \qquad (44)$$

The paramagnetic salt had a spin-lattice relaxation time of approximately 10^{-3} sec.; this dictated an upper limit

---

* A more detailed discussion of twin-T's is given by Givens and Saby (1947).

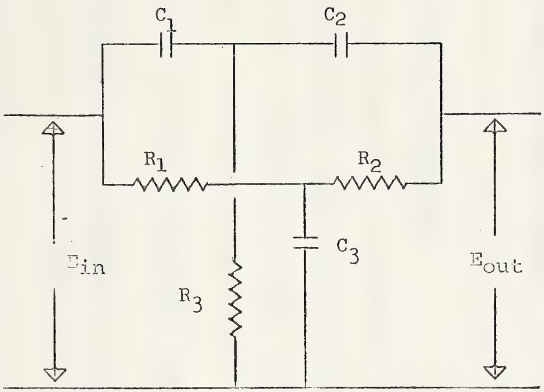

Figure 9 - Twin-T Tuning Element

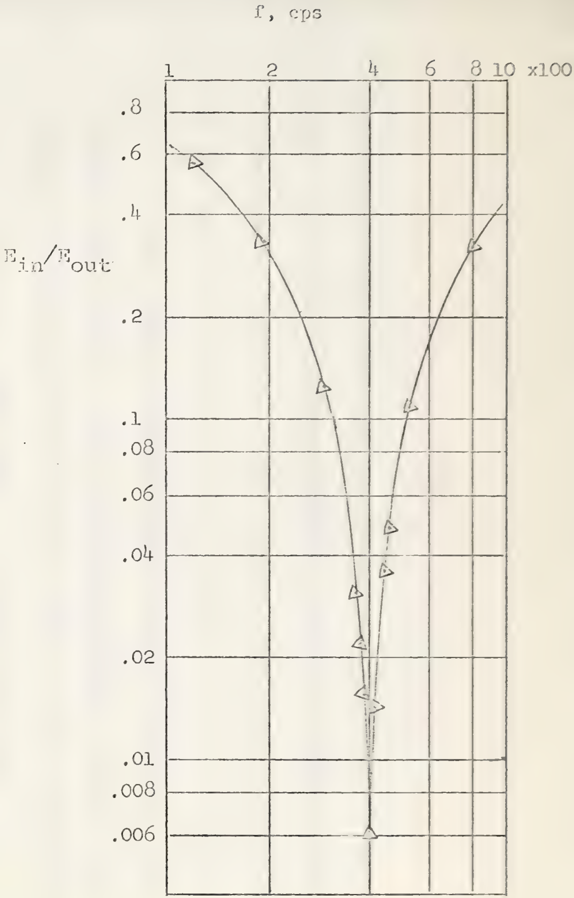

Figure 10 - Twin-T Tuning Element Response Curve

of approximately 2000 cps. At least one resonance of second sound was wanted in an experimental chamber of approximately 10 cm length; taking $u_2 = 2000$ cm/sec., this set a lower limit of 100 cps.

Using these frequency requirements in the null conditions (44), leads to the following component values, the resistors being ganged and variable from 0 to the stated value.

$R_1 = R_2 = 2000$ ohms $\qquad$ $R_3 = 1000$ ohms

$C_1 = C_2 = 1\mu f$ $\qquad$ $C_3 = 2\mu f$

A typical characteristic of a twin-T, that is, E_{out}/E_{in} vs frequency, for null condition at f_1, will have the shape shown in Figure 10.

In the amplifier, the output of this element was fed back to the original input with its voltage reversed in phase with respect to the original signal. If there is a voltage of frequency f_1 present in the original input, $E_{out}(f_1)$ will be zero; that is, there will be no feedback at frequency f_1, and a signal of this frequency will experience the full gain of the amplifier. Any voltages with frequency other than f_1 will be fed back and therefore, reduced in the final output of the amplifier.

The circuit of the complete amplifier is shown in Figure 11, and a typical response curve of the amplifier is given in Figure 12.

The response curve shown in Figure 12 was obtained under "ideal" conditions: the signal for the amplifier was derived from a voltage divider. With the input of the amplifier shorted, however, an output voltage of 400 cps was seen for almost all values of the tuning resistors. The ganged rheostats were suspected of causing the trouble, but the unwanted signal could not be eliminated. Also, it was impossible to keep the values of the ganged rheostats to within less than a few percent of what they should have been for the null condition. In additior , a fairly strong second sound signal was observed with the General Radio amplifier, but it could not be seen with the twin-T amplifier. Therefore, all the experiments employed the commercial amplifier.

The tuning element in the GR amplifier is, like the twin-T, a three-terminal network, consisting of capacitors and resistors. The tuning element is shown in Figure 13, and is described by Hall (1955).

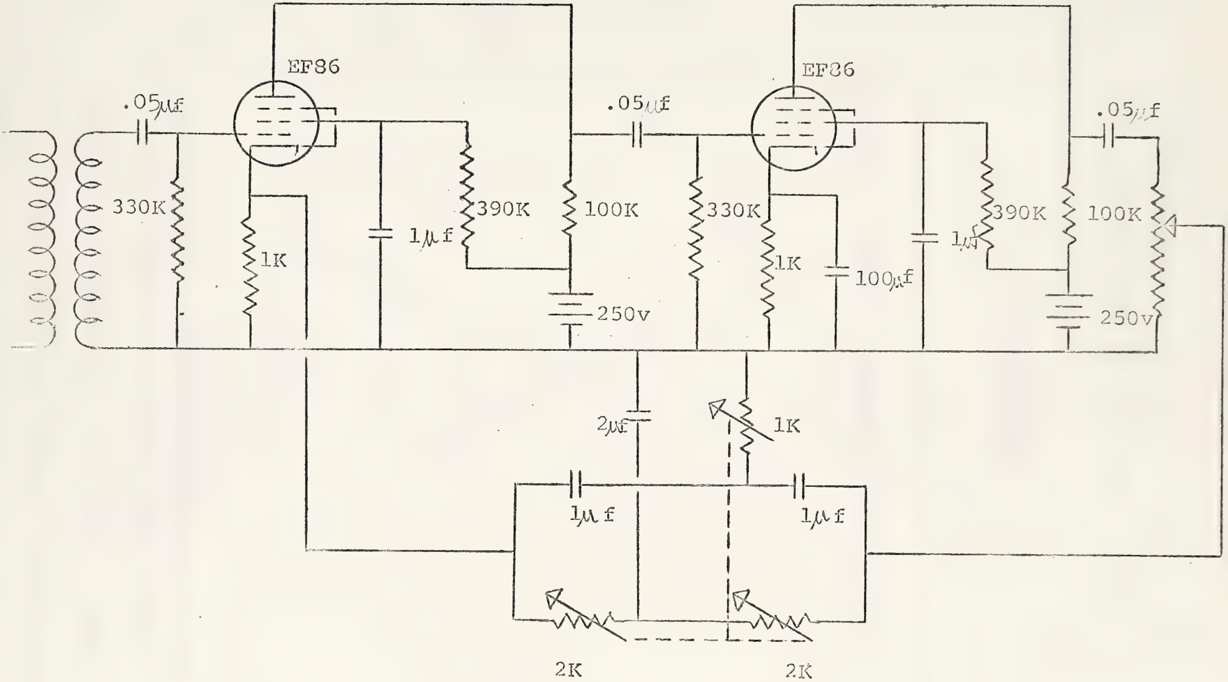

Figure 11 - Twin-T Amplifier

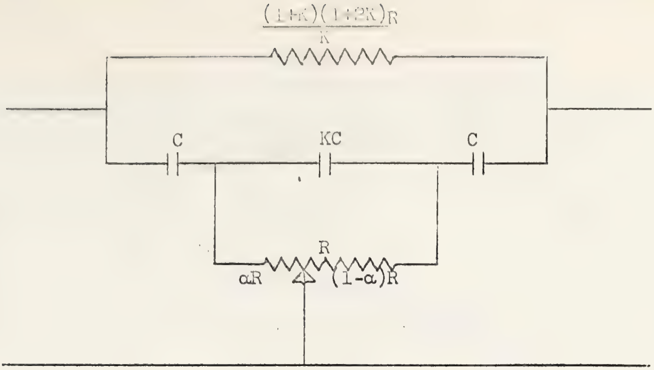

Figure 13 - Tuning Element in GR Amplifier

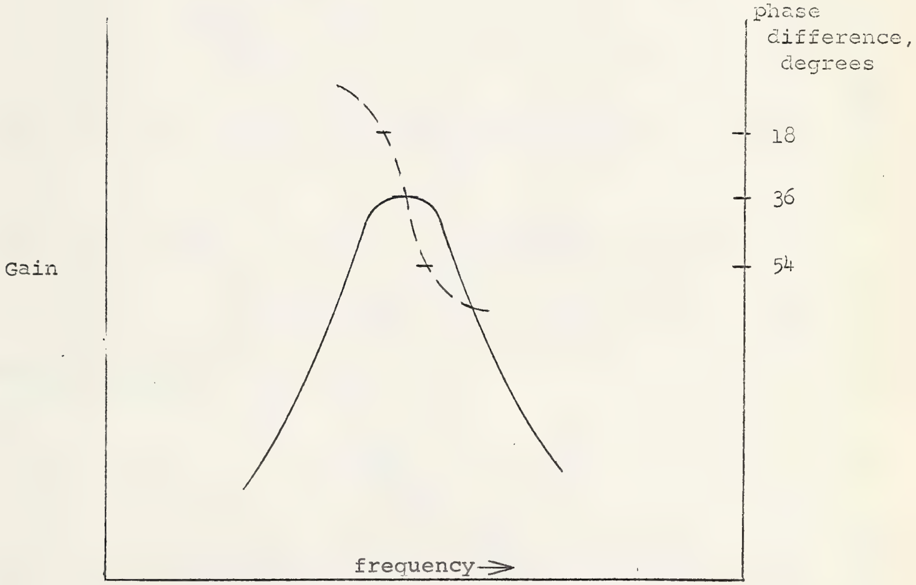

Figure 14 - Expansion of peak shown for GR amplifier in Figure 12; solid line is gain, dashed line is phase difference between input and output voltages of the GR amplifier.

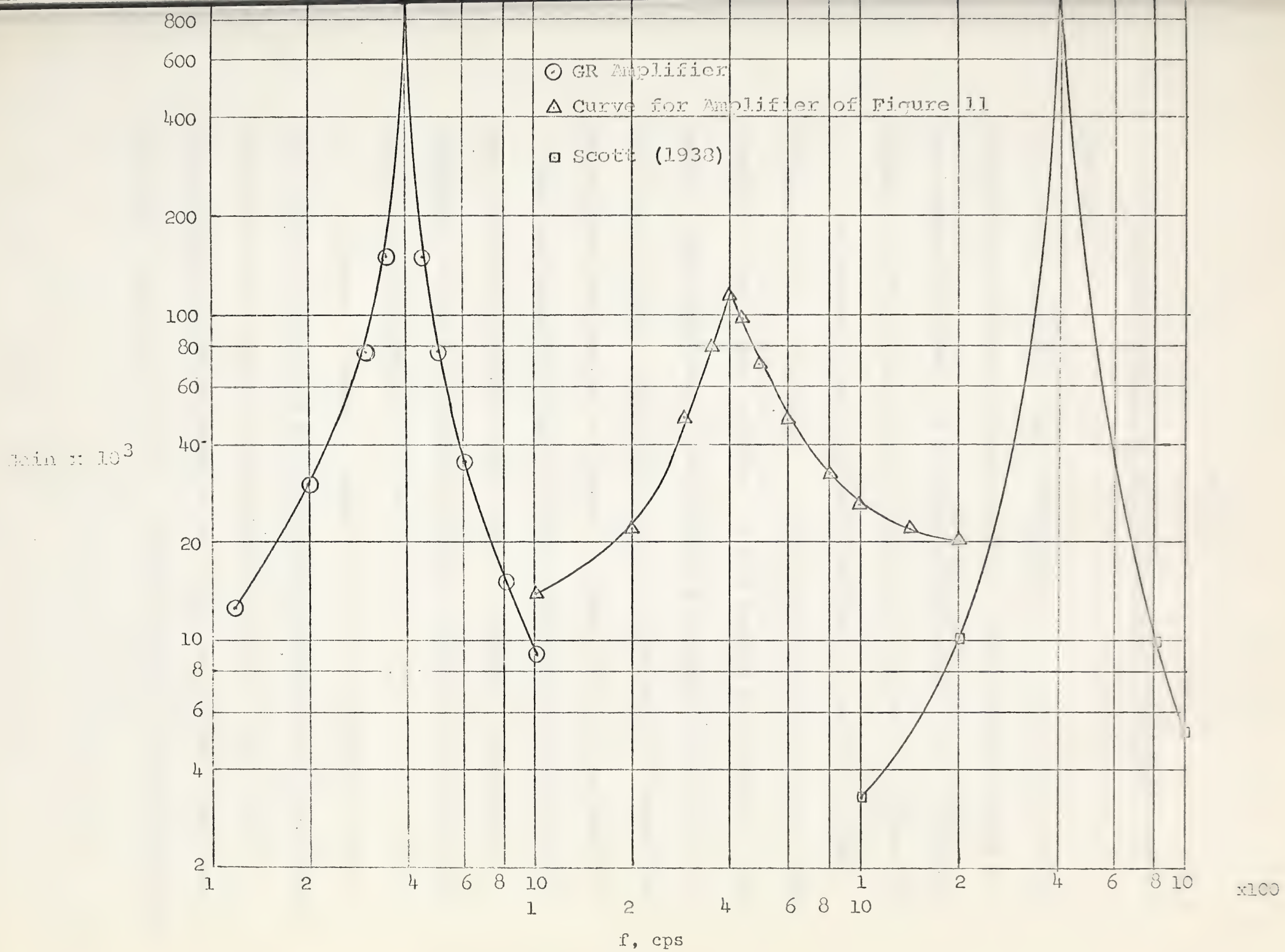

⊙ GR Amplifier
△ Curve for Amplifier of Figure 11
◻ Scott (1938)
Gain x 10^3
800
600
400
200
100
80
60
40
20
10
8
6
4
2
1
2
4
6
8
10
1
2
4
6
8
10
1
2
4
6
8
10
x100
1
2
4
6
8
10
f, cps

Figure 12

The null frequency for the element in Figure 13 is given by

$$f = \left[\alpha(1 - \alpha) \right]^{-1/2} / (2\pi RC), \tag{45}$$

for meaning of symbols see Figure 13. The response curve of the element by itself is similar to Figure 10, and a typical response curve of the entire amplifier is shown in Figure 12.

A characteristic of both the twin-T and the GR amplifiers was that the phase of the output voltage shifted (with respect to the input voltage) as the tuning was varied. This can be illustrated with the help of a graph, Figure 14; the full line is gain, the dashed is the difference in phase between input and output voltages. Figure 14 is an expansion of the peak shown in Figure 12 (for the GR), and shows the very sensitive dependence of phase on tuning. Since the operation of the PSD depended on this phase, one can see the necessity of the phase shifter.

Figure 12 shows a comparison of the response curves for the GR, the twin-T built for the second sound experiments, and the twin-T amplifier described by Scott (1938). All three amplifiers were tuned to 400 cps; it is seen that Scott's amplifier suppresses 200 cps 3 times as much as the commercial

amplifier. However, it is believed the General Radio company tried making a twin-T amplifier, but had difficulty in maintaining sufficiently high precision in the ganged rheostats to maintain satisfactory operation.

In concluding, Scott's description made the construction of a twin-T amplifier seem very worthwhile; however, his response curve could not be reproduced.

Frequency Doubler and Phase Shifter

The frequency doubler used was developed by Shepard (1953), and makes use of the fact that in the 6AS6 pentode, the amount of cathode current is controlled by the control grid, but the path of the electrons is controlled by the suppressor. When the suppressor is positive with respect to the cathode, current flow is primarily to the plate, and when the suppressor is negative, the current flow is primarily to the screen.

If a small signal, 180° out of phase with the (control) grid signal, is put on the suppressor, the resulting current flow will appear as in Figure 15.

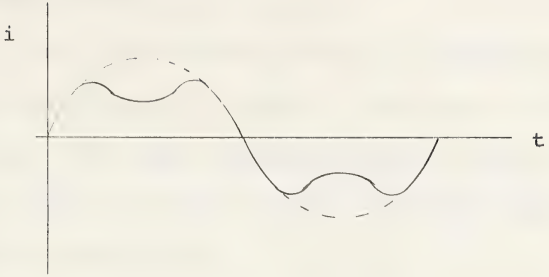

Figure 15

The dotted line is the total emission current; the full line is the plate current, and the difference between the cathode and plate currents is the screen current.

The 180° signal was obtained by grounding the suppressor and removing the by-pass capacitor from the biasing resistor; see Figure 16. The cathode now follows the grid voltage, so when the grid is increasing with respect to the cathode, the suppressor is decreasing with respect to the cathode, and this gives the 180° out of phase signal.

The output wave-form was found to be very sensitive to frequency, the magnitude of the incoming signal, and to the magnitude of B^+; the easiest way to obtain output signals with the fundamental entirely eliminated was by careful

adjustment of B^+.

The phase shifting network was adapted from one described by Howling et al (1955). The circuit is indicated in Figure 16. The main difference between this one and Howling's is that Howling used two cathode followers where I used a center-tap transformer.

Howling's vector diagram (and a straight-forward analysis) shows that: 1) the phase shift of the output voltage (with respect to the input voltage) varies from 0 to 180° as R is varied from 0 to infinity, and 2) the magnitude of the output voltage remains constant while this shift occurs. This output voltage becomes the reference voltage of the phase sensitive detector, and, as the output voltage of the PSD changes with the magnitude of the reference voltage, it is highly desirable to have the output voltage of the phase shifter constant.

The use of the transformer created a problem, because the output of the frequency doubler could be matched to the rheostat of the phase shifter only for a particular value of that resistor. Therefore, as R was changed, mismatching was produced, and the phase shifter output voltage changed.

However, a shift of approximately 150° was obtainable at all the frequencies used; the output voltage change was less than 10%, and this was not enough to affect the output voltage of the phase sensitive detector.

The transformer that was used had a primary to secondary matching ratio of 75:1; this value was picked, to some extent, by trial and error. The three capacitors in the phase shifter allowed the spanning of the frequency range 20 to 2000 cps; the largest capacitor was used for the lowest frequencies.

Three requirements called for a two-stage amplifier to be inserted between the phase shifter and the PSD:
1) some freedom as to the magnitude of reference voltage was wanted, 2) for successful operation of the phase shifter, its output could not be paralleled by an impedance of less than 1 Meg (ohm), and 3) the reference input of the PSD needed a large input voltage, and transformer coupling to the PSD dictated an input transformer; this in turn necessitated a low output impedance of the phase shifter. These goals were achieved by following the phase shifter with an amplifier of high input impedance; this amplifier was succeeded by a variable-gain cathode follower. The complete circuit is shown in Figure 16.

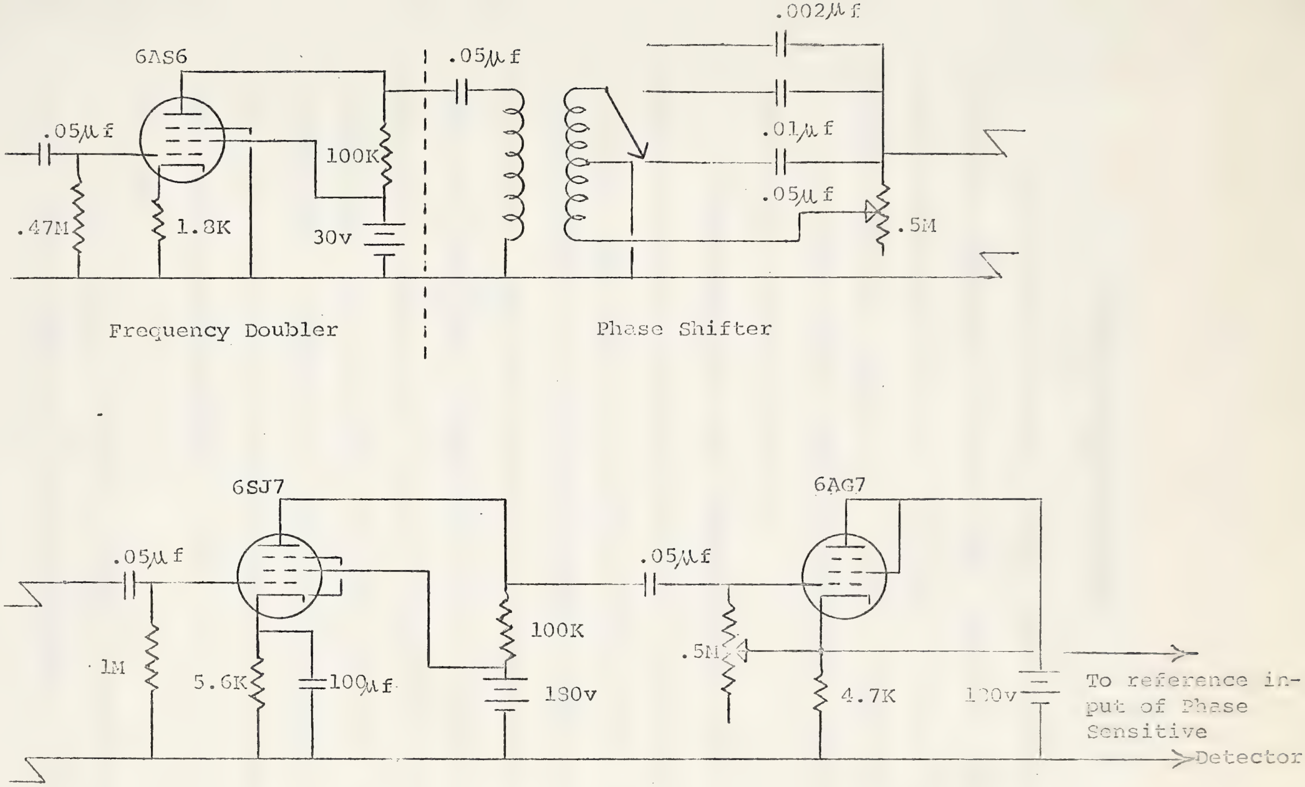
.002µf
6AS6
.05µf
.05µf
100K
.01µf
.05µf
.47M
1.8K
30v
.5M
Frequency Doubler
Phase Shifter
6SJ7
6AG7
.05µf
.05µf
100K
1M
5.6K
100µf
180v
.5M
4.7K
180v
To reference input of Phase Sensitive Detector

Figure 16

Phase Sensitive Detector

This type of amplifier is most often used to determine phase differences, Andrews (1956), page 43. Thus it is most often referred to in the literature as a phase sensitive detector, and less frequently as a "lock-in" amplifier.

The PSD used was copied after one built by Schuster (1951), and is shown in Figure 17.

Before describing the operation of the PSD, we note that the choice of the input transformer was determined by the output impedance of the cathode follower in the phase shifting circuit, and the input impedance of the grid circuits of the 6SN7. These were measured to be approximately 5K (ohms) and 30K (ohms), respectively; this called for a primary to (1/2) secondary ratio of 1:6. The closest matching in a transformer that was readily available was 1:2.4, and this worked quite satisfactorily. (Both this transformer and the one used following the frequency doubler had response curves that peaked at approximately 6000 cps, but were flat out to 5000 cps.)

The secondary produced a voltage of approximately 10 volts on each triode grid; this was sufficient to produce a

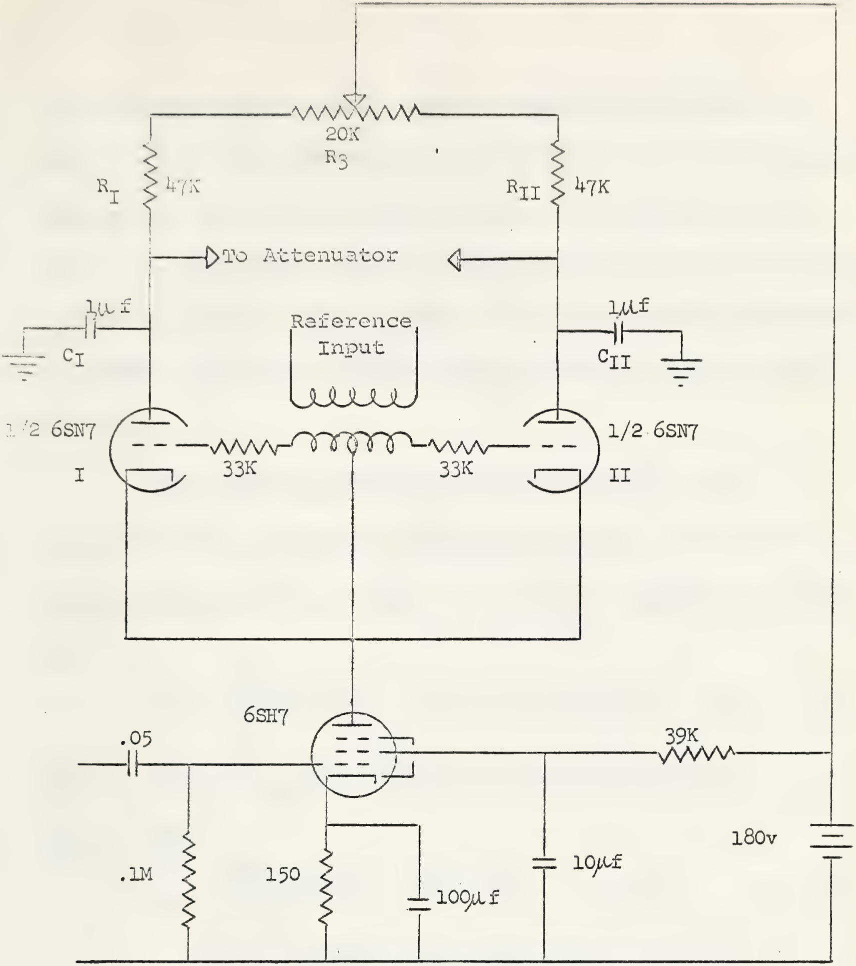

Figure 17 - Phase Sensitive Detector

switching action, that is, on the first one-half cycle of V_{ref}, tube I was conducting and tube II was cut off, and on the second half of the cycle, I was cut off and II was conducting. Since the current through a triode during its "on" period was proportional to both the signal and the reference voltages, the plate voltage of the triode was proportional to $V_s V_{ref}$.

Now, let V_{ref} equal $V_r \cos(\omega t)$, and V_{sig} equal $V_s \cos(\omega' t + \epsilon)$; ϵ will have meaning only if ω' is some integral multiple of ω. While I is on, $V_I = V_r V_s \cos \omega t \cos(\omega' t + \epsilon)$ or

$$V_I = \frac{V_r V_s}{2}\left\{\cos\left[(\omega + \omega')t + \epsilon\right] + \cos\left[(\omega - \omega')t - \epsilon\right]\right\} \qquad (45)$$

Tube II will be on 180° later, so for the second half of V_{ref}'s cycle,

$$\begin{aligned} V_{II} &= \frac{V_r V_s}{2}\left\{\cos\left[(\omega + \omega')t + \epsilon\right] + \cos\left[(\omega - \omega')t - \epsilon\right]\right\} \\ &= \frac{-V_r V_s}{2}\left\{\cos\left[(\omega + \omega')t + \epsilon\right] + \cos\left[(\omega - \omega')t - \epsilon\right]\right\} \qquad (46) \\ &= -V_I \end{aligned}$$

(The resulting expression for V_I is similar to the result of conventional amplitude modulation, except that a voltage of the carrier frequency, ω, is absent.)

The two capacitors, C_I and C_{II} act as integrators; while I is on, C_I charges, and while I is off, C_I discharges through R_I and one-half of R_3; the time constant is about 0.047 seconds. Therefore, frequencies greater than 1/0.047 or 18 cps will have little effect on the output of the PSD. Since $\omega/2\pi$ was always greater than 100 cps, the 18 cps bandwidth eliminated all voltages of frequency $\omega + \omega'$. Also, the main concern in the present set of experiments was to suppress the fundamental; the PSD did this since $(\omega - 1/2\omega')/2\pi$ was always greater than or equal to 50 cps. Occasionally, when second sound was looked for at a frequency of 200 cps, 180 cycle pickup from various laboratory power transformers was not filtered completely by the GR. In these cases, the PSD did respond slightly, but its response to a signal of 180 cps was a voltage of frequency 20 cps. Since the response time of the chart recorder following the PSD was approximately one-half second, the effective bandwidth was cut to a few cycles per second. The result was that the chart recorder responded only when $\omega = \omega'$.

So we see that $R_I + 1/2R_3$ and C_I performed time averaging; if we time-average the low-frequency component of V_I

over one cycle, we get,

$$V_I = \frac{V_r V_s}{4\pi} \int_0^{2\pi} \cos\left[(\omega - \omega')t - \epsilon\right] \, d\left[(\omega - \omega')t\right]$$

$$= \frac{V_r V_s}{2} \cos \epsilon \;\; \delta_{\omega\omega'}, \qquad (47)$$

Included in V_I will be the gain of the amplifier, g. Then

$$V_I - V_{II} = g V_r V_s \cos \epsilon \;\; \delta_{\omega\omega} \qquad (48)$$

This shows why the amplifier is sensitive to phase differences.

We can now also see why the rheostat R_3 is necessary; if the reference voltage is intentionally changed, the dc output can then be re-zeroed with this rheostat.

In practice, the dc output was proportional to V_s only up to about 2 volts, then the gain started dropping off. This problem could probably be eliminated by a change in biasing of the pentode, or by the use of a remote cut-off pentode; however, operation was satisfactory for the signals employed, so no serious effort was made to correct it.

During an experiment, when the thermometer was close to the solenoid, the induced voltage of the driving frequency was so large it overdrove the GR, and the GR output wave-form was a clipped sine wave of the fundamental frequency.

This clipping produced a Fourier compont of the doubled frequency, and the PSD responded to this. The result was that as the thermometer got closer to the Pb coil, the dc voltage increased, that is, the pen on the chart recorder drifted to one side. This problem might have been remedied by placing a filter between the thermometer and tuned amplifier. However, resonance peaks showed up superimposed on the (almost) linear drift; also, it was possible to make a substantial number of measurements with the thermometer far enough away from the coil to avoid the pickup problem.

As mentioned by Schuster, the dc drift was found to be negligible in a period of several hours. The frequencies at which this PSD was used were between 100 and 1100 cps, and a quick check showed its behaviour to be roughly constant over a frequency interval of 20 to 5000 cps; the frequency range of operation is limited by the transformers used.

Chapter 5

EXPERIMENTAL PROCEDURE

General Procedure

In all the experiments performed, the procedures for cooling the cryostat from room to liquid helium temperatures, and for calibrating the resistance thermometer, were pretty much the same.

After the thermometer, resonant chamber, and second sound generator were positioned in the experimental chamber, the inner glass can[*] was soldered on with Wood's metal, and the experimental chamber evacuated. The outer glass can was then soldered on, again using Wood's metal, and 2 was evacuated. If there were no leaks, the pressure in 2 was usually 2 x 10^{-5} torr within thirty minutes. Once it was ascertained that there were no leaks in the whole system, region 2 was valved off, and the helium dewar placed around the outer glass can. Helium gas was then admitted to 1 and 2,

---

[*] The inner and outer glass cans were both of Pyrex glass, the tops ending in Copper-glass seals, see Strong (1938), page 25.

and the pressure in 1 was noted on the Hg manometer. The dewar was filled with liquid air, and when the pressure in 1 stopped falling, the dewar was taken off, emptied, put back on and taped -- taping prevented helium from getting out, and air from getting in. The liquid air dewar was filled with liquid air, and placed around the inner dewar. A transfer siphon was then put into 3, and liquid helium was siphoned into 3. By the time the liquid level in 3 was above the needle valve, the pressure in 1 had stopped falling (that is, the contents of 1 were at 4.2°K), and the "exchange gas" in 2 was pumped out. The needle valve was opened, and 1 filled with liquid helium. The next step was to calibrate the resistance thermometer.

The resistance of the thermometer was measured with a chopper amplifier, Dauphinee and Woods (1955), and the vapor pressure was read from manometers; for pressure down to about 5 cm Hg (this corresponds to about 2.3°K), a mercury manometer was used, for lower pressures, an oil manometer was used. The temperature corresponding to a particular pressure was obtained from the tabulated values in the 1958 temperature scale, Van Dijk (1960).

Now, in order to determine the temperature amplitudes experienced by the thermometer, dR/dT had to be known as a function of T. Therefore, a plot of R vs T was made, and dR/dT could then be estimated graphically. It was desirable to have a tractable analytical expression that could give both R and dR/dT as a function of T; the two-constant equation that seems to enjoy the most success for Allen Bradley resistors is $\log R = T(a + b \log R)^2$, Clement (1955). (A list of other equations is given by de Klerk (1956), page 186, and by Barber (1961), page 154.)

For one of the resistors used in the present experiments, a plot of log R vs 1/T was found to fit a straight line fairly well; the constants were determined and the equation was $\log R = 1.459 + 1.17/T$. Then, $R = 38.8 \times 10^{(1.17/T)}$, and

$$dR/dT = -(77.5/T^2)\ 10^{1.17/T} \qquad (49)$$

A few values of T were substituted in the two preceeding equations, and found to agree quite well with estimates on the R vs T graph, so the above equations were accepted as being accurate. Equation 50 was then used for determining the temperature amplitudes shown in Table III, page 98.

Reversible Generation of Second Sound

Iron ammonium alum decomposes if it is left exposed to the air. Freshly-grown crystals were prepared in the same manner as reported by Wheatley et al (1956). This method enables fresh crystals to be kept indefinitely, and perhaps more important, the grown crystals do not stick to the glass beaker. Crystals of iron ammonium alum that were satisfactory for these experiments could be grown in one or two days by evaporation, but the resulting crystals and solution had to be heated to free the crystals from the glass.

The crystals were always ground to a coarse powder before being used as a second sound generator. This was done because a powder easily filled the lucite thimble, and because the powder seemed to have a shorter relaxation time than the crystal, see Table 2 of Benzie and Cooke (1950).

Some factors would make it easier to use whole crystals than a powder. Large crystals were more stable than the powder; freshly grown crystals were a light purple in color, and freshly ground powder was white. When crystals were taken out of the mother liquor and left in the air,

it took at least a day for a thin layer to decompose and become cloudy white. The powdered crystals, on the other hand, start turning brown in less than thirty minutes. The changes in color were thought to result from evaporation of the water of hydration.

For one of the early runs, crystals were powdered, compressed with a hydraulic press, and painted with nail varnish. Before inserting this compressed "pill" in the cryostat, one end of the pill was cut off with a knife. During this run, the magneto-resistance effect was noticed, but no resonances were observed.

After the magnitude of the magneto-resistance had been measured, the salt was again tried; but this time, after the crystals were powdered, they were lightly tamped into the thimble. (The density of the crushed salt was 1 gm/cm^3, the density of the compressed pill was 1.5 gm/cm^3, and the density of whole crystals is 1.7 gm/cm^3.) The salt was placed in position in the experimental chamber, and the inner glass can soldered on. To remove freezeable gases but keep the water of hydration from evaporating, the experimental chamber was pumped on for approximately fifteen seconds, then

liquid air was put around the outside of the glass can to freeze the water in the paramagnetic salt. After a couple of hours, the liquid air was removed, the condensed ice and water removed from the outside of the inner glass can; the outer glass can was soldered on, and the region between the inner and outer cans was pumped on for a few minutes. Liquid air was then put around the outer glass can, the vacuum pump valved off, and helium exchange gas admitted to the region between the glass cans. Small droplets could be seen on the outside of the lucite cavity; however, the salt was still white, so the cooling-down process was continued.

Resonances were observed during this run, with second sound frequencies ranging from 100 to 1100 cps. The temperature amplitudes were of the order of 10^{-5}° when the magnetic field was 480 gauss, and Kurti and McIntosh, using a compressed pill of iron ammonium alum, reported temperature amplitudes of 10^{-4}° for a magnetic field amplitude of 120 gauss. This discrepancy might arise in the method of preparation of the salt.

Filling region 3, see Figure 6, with helium from the storage dewar was often difficult; the difficulty was due to

Taconis oscillations* in this region. Once some helium was transferred, oscillations could be intentionally started (and usually stopped), but they often started with no apparent stimulus. Thin brass sheet was soldered into the cryostat in an effort to prevent the oscillations, but without noticeable effect.

The helium levels in regions 1 and 3 (see Figure 6) were periodically checked with a flashlight. When the helium level in the outer region got low, the current in the Pb coil acted as a level indicator. As part of the coil went normal, resistance appeared, and the current output of the power amplifier decreased. Occasionally, the inside of the cryostat was frosted up so much that visual checks on the liquid levels could not be made; at these times, the solenoid current was a very useful level indicator.

When tracing the temperature profile in the resonant cavity, the chart recorder pen almost always drifted to one side as the thermometer approached the paramagnetic salt. This was mainly due to clipping of the fundamental (as seen in the output of the tuned amplifier); the magneto-resistance effect did not start showing up until the thermometer was about 2 cm from the salt. This drift did not hamper measure-

---

* A discussion of Taconis oscillations is given by A. Wexler, page 155 ff, in Experimental Cryophysics. Butterworths, 1961.

ments, though, because resonance peaks were superimposed on the drift, and the "base line" for measurements of peak amplitudes was taken as the drift line. Therefore, the measurements taken of magneto-resistance were not actually needed.

At about the same position that magneto-resistance effects became noticeable, the thermometer started warming. This heating was checked a bit further. The thermometer was placed approximately 1 cm from the salt; to make sure the heating was not due to measuring current in the thermometer, the coil current was turned off. The resistance was then measured with 10 microamps, and with 200 microamps; the current was left on for about thirty seconds, and in both cases R stayed at 239 ohms (which corresponded to 1.27°). The magnetic field was turned on, and in a few seconds, R decreased to 233 ohms (1.29°), and stayed at this value as long as the magnetic field was on. The magnetic field amplitude at the thermometer was approximately 270 gauss, and the frequency was 250 cps. Since this heating presented no problems, it was not investigated any further.

Chapter 6

RESULTS

Magneto-Resistance

The high-field magneto-resistance results are shown in Figure 18; it is seen that above 6 kgauss, the change in resistance was roughly proportional to H^2, which agrees with other investigators, (Clement and Quinell (1952)).

The low-field magneto-resistance is shown in Figure 19. It is possible that static field measurements would not give the same results as shown in Figure 19. If the change in resistance were actually given by, say,

$$R = a_1(T)H + a_2(T)H^2 + a_3(T)H^3, \tag{50}$$

then the a.c. measurements presented here would be measuring only $a_2(T)$; and this is because the tuned amplifier was tuned to twice the driving frequency.

As was stated on page 35, the chopper amplifier was used to measure resistance changes for the high-field measurements and the second sound apparatus for the low fields. The chopper amplifier was barely able to resolve resistance changes of 0.1 ohm, but the a.c. method resolved changes of 0.015 ohms easily. These a.c. measurements were made with the GR

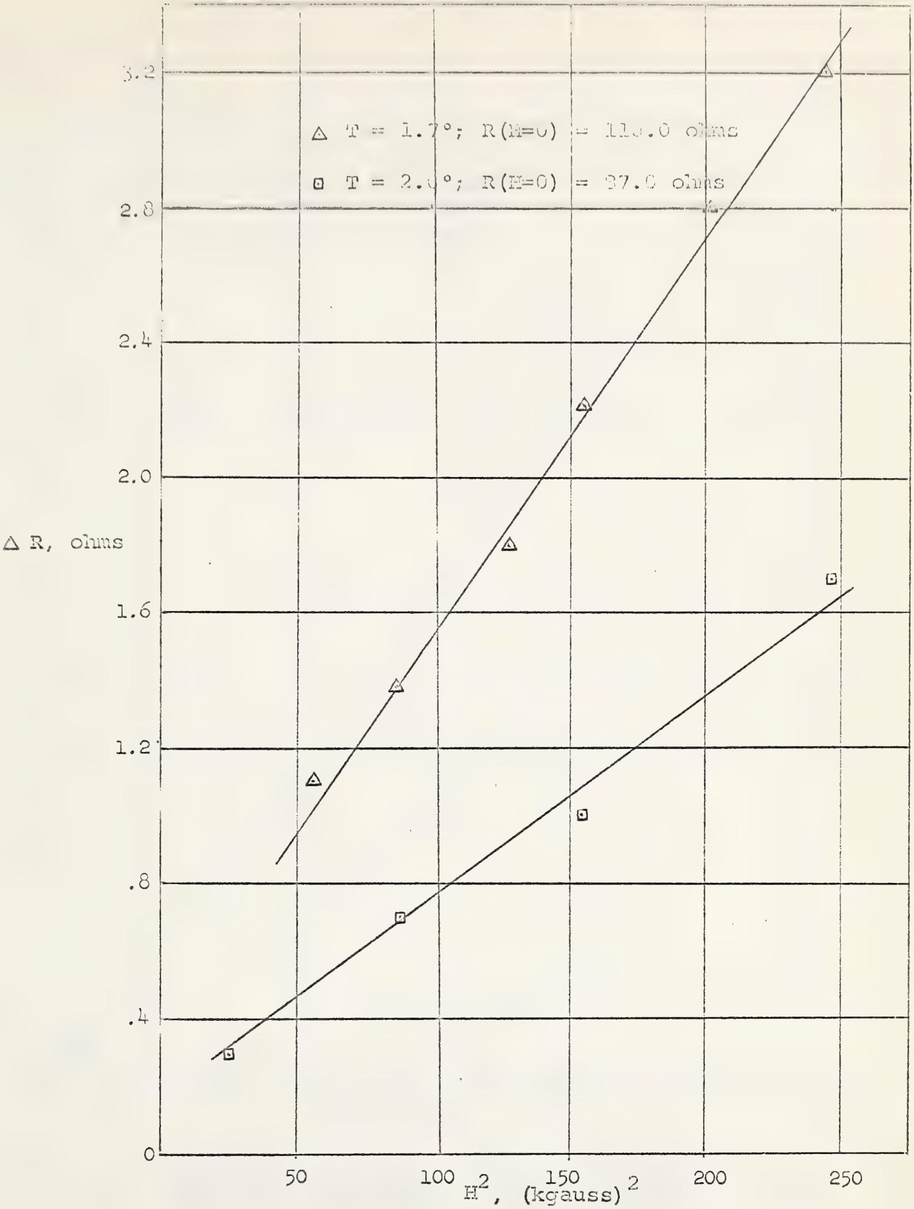

Figure 18 - High-Field Magneto-Resistance. △ R is the change from the zero-field value.

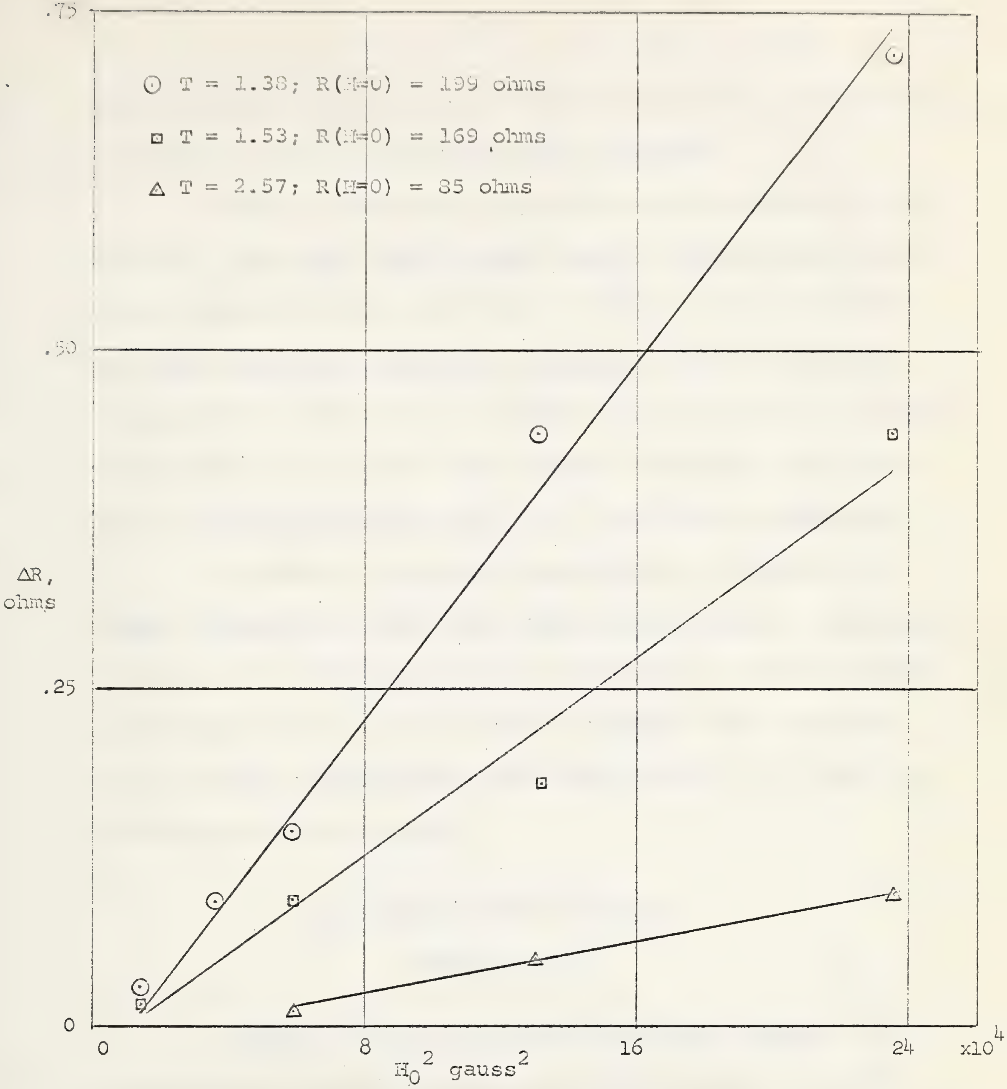

Figure 19 - Low-Field Magneto-Resistance. ΔR is the change from the zero-field value.

tuned amplifier only; had the PSD also been used, even smaller resistance changes would have been detectable.

Since voltages of 0.1 microvolt were positively detected with the tuned amplifier-PSD set up, the detectable resistance change is given by $R = V/I = 10^{-7}/I$. Therefore, the minimum detectable resistance change will be determined by the maximum amount of d.c. current that can be used. In these experiments, $I = 2 \times 10^{-4}$ amps caused no heating; this means that a resistance change of 5×10^{-4} ohm could be detected.

In static, high-field measurements of magneto-resistance, Hornung and Lyon (1961) were able to measure resistance change of 1×10^{-4} ohm. However, they did not describe their measuring circuit, so it is hard to compare the sensitivity of the tuned amplifier-PSD technique with the d.c. method employed by Hornung and Lyon.

Irreversible Generation of Second Sound

The main reason for using a resistance heater was to determine the feasibility of employing a ground-down Allen Bradley resistor as a thermometer for second sound. The

frequency response was determined, and the signal voltage for a limited range of heater currents was observed.

For a constant heater current, there was a wide scatter of points on a temperature-amplitude vs frequency plot, but no trend of decreasing response with an increase of frequency up to 1400 cps. No trend would be expected if equation (36) gives the correct thermal skin depth.

The plot of temperature amplitude vs heater power did not give a predictable result: one would expect the temperature to vary linearly with the power input to the heater. Peshkov (1948) observed a very noticeable departure from linearity; the present experiment did not employ a wide enough range of heater current to plot a very full curve. The data obtained by Peshkov and the data obtained in this experiment are shown in Figure 20. There appears to be no explanation for the anomaly observed by Peshkov; it is obvious that more data would be necessary to make a comparison with Peshkov's results.

Quantitative measurements on the temperature dependence of the velocity of second sound were not made. However, it was noticed during the run

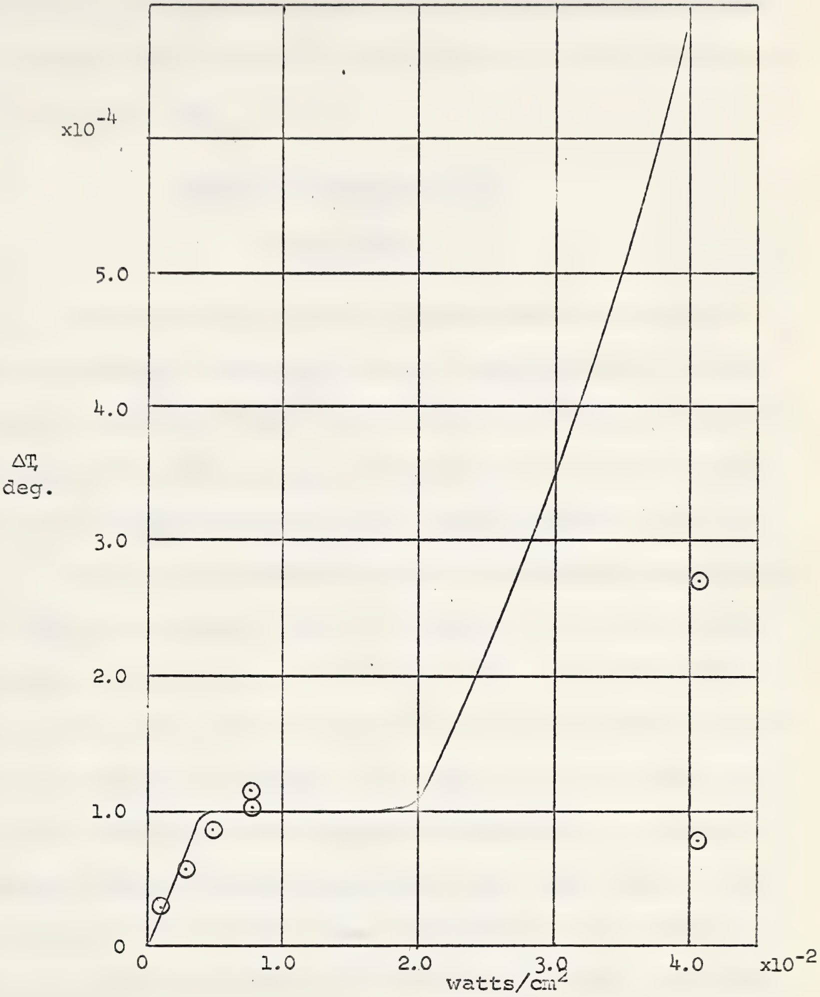

Figure 20 - Temperature amplitude vs power input to heater for irreversible generation of second sound. Solid line data from Peshkov (1948); ⊙ - data from this experiment.

employing the resistance heater that a change in the position of resonance peaks resulted from a change in bath temperature of less than 0.1°K.

Reversible Generation of Second Sound

Measurements on several properties of the paramagnetic salt-helium system were made. The velocity of second sound was measured; the effect of the spin-lattice relaxation was looked for; and a value for attenuation of second sound was obtained from measuring the "Q" of the resonant cavity.

One of the problems in making measurements was due to the characteristics of the chart recorder. The recorder's response time was slower than that of the rest of the detection electronics; and the pen of the chart recorder displayed a small "hysteresis" effect: the input to the recorder was shorted, and the pen was allowed to stop moving. A small positive voltage was then applied to the input, and the pen allowed to come to rest. When the input was again shorted, the pen never did return to its original position. The difference in pen position was at most 5% of the total chart

width, but it made looking for small signal differences difficult.

These two characteristics -- slow response time, and hysteresis of pen position -- were probably the limiting factors in making accurate velocity measurements. If there had been no hysteresis, the most accurate method would be to locate a resonance peak, and then move the thermometer up and down until a maximum deflection was obtained. This would necessitate adjustment of the phase shifter, because the phase changes as a resonance is traversed. Once maximum deflection was found for a resonance peak, the position of the thermometer would be noted (the thermometer was attached to vernier calipers, and the calipers could be read to 0.1 mm). The phase would change by exactly 180° at the next resonance, so the phase shifter would not be adjusted, but the maximum deflection would have to be found.

The method that was used for almost all of the velocity measurements consisted of pushing the thermometer slowly and steadily down (or up) the resonant cavity, and marking on the chart record the caliper reading every centimeter or half-centimeter, cf Figure 21. The current in the thermometer was

then switched off, but the magnetic field left on, and the same path was traced by the thermometer -- in this way, the deflection on the recorder that was due to induction pickup was obtained, see Figure 22. To get the deflection due to second sound, the readings on records like that in Figure 22 were subtracted from the corresponding records (as in Figure 21).

The accuracy of this method is obviously limited by how constant the velocity of the thermometer was, and by how closely the marked position on the chart coincided to the actual thermometer position.

A complication that arose in all measurements was that of correct adjustment of the phase shifter. When the thermometer was far from the Pb coil, resonances were sometimes strong enough that the correct phase could be determined by means of a straight-line Lissajous figure. In the more common situation of weak signals, phasing was determined by maximum deflection on the chart recorder.

Another problem was the presence of the magnetic field. It caused a drift due to both clipping of the harmonic in the tuned amplifier, and to magneto-resistance. As has been mentioned, these effects did not become noticeable until the

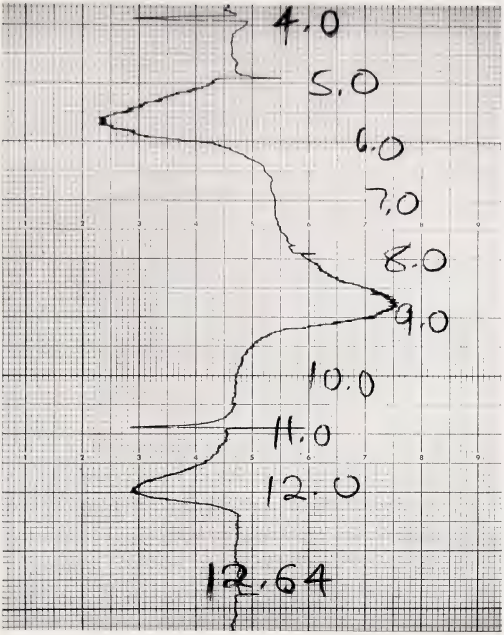

Figure 21

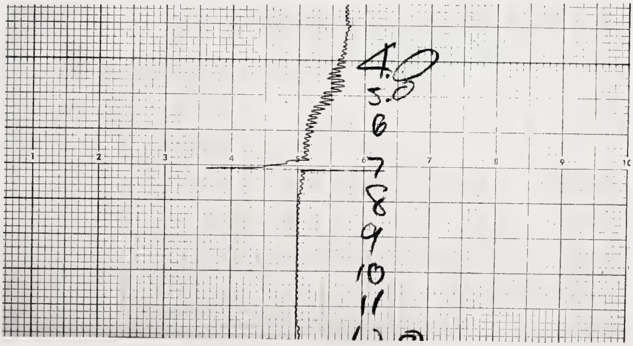

Figure 22

thermometer was less than 2 cm from the salt. In the (second sound) frequency range from 300 to 500 cps, there was very little drift, but at frequencies less than 300 and above 500 cps, there was a great deal of drift. It usually was not possible to tell magneto-resistance from induction pickup, and this "quiet" frequency range of 300 to 500 cps might be due to a cancellation of the two effects.

Photographs of the chart record for second sound frequency of 300 cps, and T = 1.30°K, are shown in Figure 21. This trace illustrates several aspects.

The first resonance was a half-wavelength from the source. The thermometer was mounted such that a caliper reading of 3.0 meant the thermometer was 2.5 cm from the salt. The record shows the first resonance at a caliper reading of 5.7 cm, or 3.3 cm from the salt. At 1.3°K, Peshkov (1960) gives u_2 = 1970 cm/sec. $\lambda/2$ is then equal to 3.3 cm.

The first resonance at $\lambda/2$ is the same as is observed in ordinary sound, i.e., the first pressure antinode in a first sound resonator would occur at $\lambda/2$. In first sound, positions of pressure antinodes are positions of particle-displacement nodes, i.e., pressure and particle-displace- antinodes are separated by a distance of $\lambda/4$. The same

separation (in the longitudinal mode) occurs in second sound; temperature and particle-displacement antinodes are $\lambda/4$ apart. For second sound this can be seen from the following. Dingle (1948) shows that He_{II} obeys the equation

$$\partial v_n / \partial t + s \rho_s \nabla T / \rho_n = 0, \tag{51}$$

where s = entropy/gm. The temperature distribution at resonance is given by

$$T = T_0 \cos \omega t \cos kx, \tag{52}$$

where the spatial origin is taken at the salt. We know from (3) that v_n and v_s are 180° out of phase; to find v_n; solve for v_n in (51), using (52): $\partial T/\partial x = -kT_0 \cos \omega t \sin kx$; therefore,

$$v_n = -T_0 \, s \, \rho_s / \rho_n u_2 \ \sin kx \sin \omega t, \tag{53}$$

and

$$x_n = T_0 s \, \rho_s / (\rho_n u_2 \omega) \ \sin kx \cos \omega t. \tag{54}$$

From (54) and (52), we see that particle-displacement and temperature antinodes are separated by $\lambda/4$. That these conditions do hold has been demonstrated with the thermal Rayleigh disk, (Pellam (1955)).

Also, from (52), we see that successive resonances should be 180° out of phase; this is quite evident from

Figure 21. (52) also states that successive resonances should be separated by a distance of $\lambda/2$. The bath temperature was 1.3°; at this temperature, u_2 = 1970 cm/sec, Peshkov (1960). The second sound frequency was 300 cps; therefore, $\lambda/2$ = 3.3 cm. The observed peak separations, starting at the caliper reading of 5.7, were 3.3, 3.0, and 3.3 cm.

These separations correspond to values for u_2 of 1980, 1800, and 1980 cm/sec., making an average of 1920 cm/sec. This average is within 2% of the accepted value; however, the other measurements were not so close. The average value, obtained from 12 traces similar to Figure 21, was 2065 cm/sec, at 1.38°K. The standard deviation was ±10 cm/sec; Peshkov gives u_2 = 1960 cm/sec. at 1.38°.

From Figure 21, we can also get a measurement of temperature amplitudes. After the trace (Figure 21) was obtained, the chart deflection was calibrated with the voltage divider, Figure 7; the result was 2.2 inches/ micro-volt. To obtain temperature amplitudes, the "pickup" values (obtained with the thermometer current turned off) of Figure 22 were subtracted from the readings in Figure 21; this gave the true peak heights. The voltage developed across the thermometer

was obtained from the above calibration, and the temperature amplitude calculated from $\Delta T = \dfrac{V}{I\ dR/dT}$. For this particular trace $I = 2 \times 10^{-4}$ amp, and $dR/dT = 365$ ohm/deg. The results are summarized in Table III.

Peak No.	Caliper Reading	Chart Deflection	Pick-up Deflection	Actual Peak Height	$V_{ther.}$	Temp. Amplitude
1	5.7	2.3	5.5	3.2	$3.3\text{x}10^{-6}$	$4.5\text{x}10^{-5}$
2	8.7	7.5	5.0	-2.5	$2.7\text{x}10^{-6}$	$3.7\text{x}10^{-5}$
3	12.0	2.9	5.5	2.1	$2.3\text{x}10^{-6}$	$3.2\text{x}10^{-5}$

Table III

The above values are representative of temperature amplitudes obtained at other frequencies during this run for the same bath temperature and magnetic field; peaks that were measured ranged in temperature amplitude from 5×10^{-5} to 1×10^{-5}°. The magnetic field amplitude at the salt was 360 gauss.

To compare predicted and observed temperature amplitudes, we use f = 150 cps, $H_0 = 360$ gauss, T = 1.3°, and $\tau = 10^{-3}$ sec.; equation (29) then becomes

$$T_H = 3 \times 10^{-4} \beta \text{ deg.} \qquad (55)$$

where β is the thermal skin depth in cm. Before a value of β is inserted in (55), it must be kept in mind that the resonator will produce some increase in amplitude above that given by (55), i.e., if the waves had been freely travelling instead of in a resonator, the values for amplitudes would be less than those given in Table III.

Therefore, a value of 0.1 to 0.01 cm for β would give good agreement between (55) and the values in Table III. Also, the salt was in the form of loosely packed granules, and the granule size was roughly 10^{-2} cm. Intuitively, one would expect the skin depth to be no larger than the granule size. So the values for β that make agreement between (55) and the experimental results seem quite reasonable.

Kurti and McIntosh (1955), using a compressed pill of the same paramagnetic salt,reported temperature amplitudes of approximately 10^{-4}°. However, they said only that they used frequencies between 150 and 1200 cps, the maximum H_0 was 120 gauss, and that the temperature amplitude increased rapidly with decreasing temperature. The fact that they observed an amplitude 10 time as large as those shown in Table III

indicates that either the handling of the salt was important, or that my resonator geometry was not as efficient as theirs.

From Figure 21, we can also find the attenuation of second sound. The attenuation constant, α, is defined by the equation of a travelling second sound wave, $T = T_0 \exp(-\alpha x)\cos(\omega t - kx)$; α can be shown to be related to the Q of the cavity by

$$\alpha = 2\pi/\lambda Q, \tag{56}$$

where Q is defined to be $2\pi\left(\frac{\text{energy stored}}{\text{energy dissipated/cycle}}\right)$, see Kittel (1947), page 229. $Q = f/\Delta f$, and $2\Delta f$ is the width of the resonance curve at the point where the amplitude is $1/\sqrt{2}$ of its maximum value. In these experiments, the frequency was held fixed, and the resonance curves obtained by varying the length of the cavity. Therefore, Q was obtained from

$$Q = \lambda/\Delta l \tag{57}$$

and $2\Delta l$ is the half width defined above. From Figure 21, the Q's corresponding to the T's of Table III are,

$$Q_1 = 22$$
$$Q_2 = 20 \tag{58}$$
$$Q_3 = 33.$$

If (56) is written in a slightly different form, a comparison between the values shown in (58) and the results obtained by other authors can be made.

$$\alpha = 2\pi / \lambda Q \qquad (56)$$

or

$$\alpha/\omega^2 = 1/(2\pi Q f u_2) \ \ \mathrm{sec}^2/\mathrm{cm} \qquad (59)$$

At 1.31°K, Zinov'eva (1957) obtained $\alpha/\omega^2 = 1.2 \times 10^{-12}$. Therefore, Zinov'eva's Q at 300 cps would be $Q_{Zin} = 2.3 \times 10^5$. Snyder (1961) obtained a Q of 2000 for a frequency of 1 kc; since Qf is a constant, Snyder's Q at 300 cps would be $Q_{Sny} = 6700$.

Qf is a constant because

$$\alpha/\omega^2 = 1/(2\rho u_2^3)\left\{\rho_s/\rho_n\left[4/3\eta_n + \zeta_2 - \rho(\zeta_1 + \zeta_4) + \rho^2\zeta_3\right] + \chi/C\right\}, \qquad (60)$$

where η and the ζ's are coefficients of viscosity, χ is the thermal conductivity of the normal component and C is the specific heat; see Atkins (1959), page 156. None of the quantities on the right hand side of (60) is a function of frequency, therefore, the right hand side of (59) is a constant at a particular temperature, and thus, Qf is also constant.

Snyder's resonant chamber was rectangular, and made

of Lavite. My cylinder was made of lucite; one of the reasons for the low Q obtained in my resonator was energy lost by radiation through the space between the thermometer backing and the cylinder wall.

If the thermometer had been moved rapidly, turbulence would have been introduced; this would probably affect the Q of the cavity and the temperature amplitudes. An estimate of the linear velocity of the thermometer necessary to produce turbulence can be obtained from the Reynolds number of He_{II}. The Reynolds number is defined by

$$R = (v_c \rho \lambda / \eta), \tag{61}$$

where v_c is the velocity at which turbulence sets in, ρ is the density of the fluid, η is the viscosity of the fluid, and λ is the penetration depth of "viscous waves". Results obtained with oscillating cylinders give $R = 220$, $\rho/\eta \simeq 10^4$ sec./cm^2, $\lambda \simeq 0.3$ mm; see Lane (1962), page 47; and Atkins (1959), page 196. Solving (61) for v_c yields $v_c \simeq 1$ cm/sec. When tracing resonance peaks, the thermometer velocity was approximately 1.2 inches/minute, or 0.05 cm/sec. Therefore, we can discount turbulence.

APPENDIX I

ALTERNATE APPROACH FOR OBTAINING TEMPERATURE AMPLITUDES

On pages 20 - 30, the temperature amplitude was arrived at in a method similar to that used for a resistance heater; that is, the energy supplied to the heater was determined by first considering the heater to be thermally isolated from the helium. Then the effect of the helium on the heater was accounted for by way of the impedance of the helium.

Another approach can be used. If we start with a low enough frequency such that the spins, the lattice, and the helium are all in thermal equilibrium, an expression for the resulting temperature amplitude can be obtained thermodynamically, without recourse to the impedance of the helium.

The thermodynamic system is now the spin system, the lattice, and the helium. The Tds equation for this system is

$$Tds = c_s dT + T(\partial M/\partial H)_T dH + c_l dT + c_H dT, \tag{62}$$

where the first two terms on the right hand side of (62) are contributions from the spin system, the third term is due to the lattice, and the fourth term is due to the helium.

In a second sound experiment, the system described above is, to a very good approximation, thermally isolated from its surroundings. Therefore, ds in (62) is zero, and dT is given by

$$dT = \frac{bHdH \times 10^{-7}}{T(c_s+c_l+c_H)} \cdot \tag{63}$$

Comparing the magnitudes of the specific heats,

$$\left.\begin{aligned} c_s &= 4.8 \times 10^{-4}/T^2 \quad \text{joules/cm}^3\text{-deg.} \\ c_l &= 10^{-5}T^3 \quad \text{joules/cm}^3\text{-deg.} \end{aligned}\right\} \tag{7}$$

$$c_H = 1.6 \times 10^{-2}T^{6.7} \quad \text{joules/cm}^3\text{-deg.,}$$ Daunt and Smith (1954), page 190; we see that c_s and c_l can be ignored in (63).

To obtain the temperature amplitude from (63), we integrate over one quarter period of H. Since $H = H_0\exp(i\omega t/2)$, $dH = (iH_0/2)\ \exp(i\omega t/2)\ d(\omega t)$. Therefore,

$$T_H = \frac{ibH_0^{\ 2}}{2c_HT} \int_0^{/2} e^{i\omega t}d(\omega t)\text{, or,}$$

$$T_H = \frac{bH_0^{\ 2} \times 10^{-7}}{2Tc_H} \ \text{deg.} \tag{64}$$

and for iron ammonium alum,

$$T_H = H_0^{\ 2} \times 10^{-7}/T^{7.7}. \tag{65}$$

This model makes no provision for the spin-lattice relaxation effect, and no easy method is seen in which this effect can be taken into account.

To compare the two approaches with each other and with experimental results, we rewrite equations (29) and (65).

$$T_H = \frac{\omega b H_0{}^2 \beta \times 10^{-9}}{T^{5.6}(1 + \omega^2\tau^2)^{1/2}} \text{ deg.} \tag{29}$$

$$T_H = H_0{}^2 \times 10^{-7}/T^{7.7} \text{ deg.} \tag{65}$$

For $f = 150$ cps, $H_0 = 360$ gauss, $T = 1.3°$, and $\tau = 10^{-3}$ sec., (29) gives $T_H = 3 \times 10^{-4}\beta$ deg., and (65) gives $T_H = 1.7 \times 10^{-3}°$. The experimental value is $5 \times 10^{-5}°$. However, for several reasons, significant conclusions cannot be drawn.

First, a very rapid increase in temperature amplitude for decreasing temperature was noticed both by Kurti and McIntosh and by myself; however, measurements were not made that would allow a distinction between the temperature dependences of (29) and (65). Second, Kurti and McIntosh observed temperature amplitudes of $10^{-4}°$ with a magnetic field of 120 gauss, and roughly the same temperature and frequency as mentioned above. Evaluating (29) and (65) with these values of

frequency and magnetic field gives a prediction of temperature amplitudes of roughly 10^{-4}°; however, the amount of amplification produced by Kurti and McIntosh's chamber is not known.

Therefore, all one can say is that more careful measurements would have to be made to distinguish which of the two approaches provide a better physical description of the experimental situation.

APPENDIX II

SEARCH COIL

From the measured geometry of the search coil mentioned on page 41, and Faraday's law of induction, it was calculated that when the coil was in a field of B gauss and frequency f, the voltage across the coil should be

$$V = 5.77 \times 10^{-6} fB \text{ volts.} \qquad (66)$$

The numerical coefficient was checked by placing the search coil in a long solenoid of 600 turns/meter, measuring the current through this standard solenoid by looking at the voltage developed across a standard 1-ohm resistor with a scope. The field inside the standard solenoid was assumed to be given exactly by $B = \mu_0 ni/l$, where the symbols have the usual meanings.

With the search coil in the standard solenoid, and a known current passing through the standard solenoid, the voltage across the coil was measured for various frequencies and fields; since an oscilloscope was used, all readings were peak to peak.

These voltages were then compared with the values calculated from (66). The largest discrepancy was 3%, and

there were no systematic differences; therefore, (66) was taken to be correct. To facilitate the use of this search coil in calibrating other solenoids, a graph of B vs V was drawn for f = 100 cps; the slope was 1.72 gauss/millivolt.

The search coil was mounted on a swivel, and then on the end of a long brass rod. Long twisted leads (which were found to have no effect on the calibration) were run from the coil out to the end of the rod. This arrangement enabled fields at almost any angle to the rod's axis to be measured.

SUMMARY

The main goal of this thesis project, to develop the technical aspects of reversible second sound generation and detection, has been accomplished.

Calculations to explain the observed temperature amplitudes have been made using two different approaches. The agreement with experimental data is fairly good; however, more information on the thermal depth of the salt (see equation 17) would be desirable. The calculations give a quantitative account of factors influencing temperature amplitudes which were only mentioned in the earlier work of Kurti and McIntosh (1955).

Electronics have been described that were built for this thesis, and which are capable of detecting a voltage of 0.1 microvolts in the low audio frequency range.

Experimental measurements have been made on both low-field (less than 1 kgauss) and the conventional high-field magneto-resistance of an Allen Bradley resistor-thermometer. A comparison of irreversibly-generated second sound temperature amplitudes has been made with results obtained by Peshkov; and with the reversible generator, limited measurements on the

velocity and attenuation of second sound have been presented.

In addition, a possible method for studying spin-lattice relaxation times in paramagnetic salts has been suggested, and a method for exciting radial modes of second sound in a cylindrical resonator has been mentioned.

BIBLIOGRAPHY

Anderson, A.C., Salinger, G.L., Steyert, W.A., and Wheatley, J.C.; Phys Rev Letters, 6, 331, (1961).

Andrew, E.R.; Nuclear Magnetic Resonance, Cambridge University Press, 1956.

Atkins, K.R.; Liquid Helium, Cambridge University Press, 1959.

Atkins, K.R., and Hart, K.H.; Can Jour Phys 32, 381, (1954).

Badlidze, R.A.; Sov Phys JETP (English*) 16, 1476, (1963).

Barber, C.R.; Progress in Cryogenics, Vol 2. Heywood and Company, 1960.

Bardeen, J. and Schrieffer, J.R.; Progress in Low Temperature Physics, Vol 3, Chapter 6. North Holland Publishing Company, 1960.

Benzie, R.J. and Cooke, A.H.; Phys Soc Proc A63, 201, (1950)

Berman, R.; Phys Soc Proc, 1029, (1952).

Bloor, D.; Problems of Low Temperature Physics and Chemistry, Vol 2. Permagon Press, 1960.

Carslaw, H.S. and Jaeger, J.C.; Conduction of Heat in Solids, 2nd ed., Oxford University Press, 1959.

Casimir, H.B.G. and du Pre, F.K.; Physica 5, 507 (1938).

Chester, M.; Phys Rev 131, 2013, (1963).

Clement, J.R.; Temperature, Its Measurement and Control in Science and Industry, Vol 2. Reinhold, 1955.

---

* This refers to the English translation of the Russian journal.

Clement, J.R. and Quinnell ,E.H.; Rev Sci Instr 23, 213, (1952).

Clement, J.R., Quinnell , E.H., Steele, M.C., Hein, R.A., and Dolecek, R.L.; Rev Sci Instr 24, 545, (1953).

Cooke, A.H.; Reports on Progress in Physics 13, 276, (1950).

Daunt, J.G. and Smith, R.S.; Rev Mod Phys 26, 172, (1954).

Dauphinee, T.M. and Woods, S.B.; Rev Sci Instr 26, 693, (1955).

Dessler, A.J. and Fairbank, W.M.; Phys Rev 104, 6, (1956).

van Dijk, H.; Progress in Cryogenics, Vol 2, p. 121, Heywood and Company, Ltd., 1960. For a tabulation of various pressure-temperature relations from the 1958 temperature scale, see the National Bureau of Standards Monograph 10, U.S. Department of Commerce.

Dingle, R.B.; Phys Soc Proc 61, 9, (1948).

Dingle, R.B.; Phys Soc Proc A65, 1044, (1952)

Fairbank, H.A. and Lane C.T.; Rev Sci Instr 18, 525, (1947).

Ginzburg, V.L.; Sov Phys JETP (English*) 14, 594, (1962).

Givens, M.P. and Saby, J.S.; Rev Sci Instr 18, 342, (1947).

Golovashkin, A.I. and Motulevich, G.P.; Instrum Exper Tech (English*) 2, 404 (1962).

Gorter, C.J.; Progress in Low Temp Phys, Vol 1, p. 8, North Holland Publishing Company, 1955.

Hall, H.E. and Vinen, W.F.; Roy Soc Proc A238, 204, (1956).

Hall, H.P.; I R E Transactions on Circuit Theory, Vol CT-2, No. 3; p. 283, Sept. 1955.

---

* This refers to the English translation of the Russian journal.

Hanson, W.B. and Pellam, J.R.; Phys Rev 95, 321, (1954).

Hassan, A.; M.Sc. thesis, University of Alberta, Edmonton, 1961.

Hornung, E.W. and Lyon, D.N.; Rev Sci Instr 32, 684, (1961).

Howling, D.H., Mendoza, E., and Zimmerman, J.E.; Roy Soc Proc A229, 86, (1955).

Hudson, R.P.; Experimental Cryophsics, chapter 9. Butterworths, 1961.

Jahnke, E. and Emde, F.; Tables of Functions, Dover, 1945.

Keesom, P.H. and Pearlman, N.; Phys Rev 99, 1119, (1955).

Kittel, C.; Reports on Progress in Physics 11, 205, (1946-47).

de Klerk, D., Hudson, R.P. and Pellam, J.R.; Phys Rev 93, 28, (1954).

de Klerk, D.; Handbuch der Physik 15, p. 38. Springer, 1956.

Kurti, N. and McIntosh, J.; Phil Mag 46, 104, (1955).

Kunzler, J.E., Geballe, T.H., and Hull, G.W.; Rev Sci Instr 28, 96, (1957).

Landau, L.; Jour Phys USSR 5, 71,(1941).

Lane, C.T.; Superfluid Physics, McGraw-Hill, 1962.

Little, W.A.; Phys Rev 130, 596, (1963).

London, F.; Superfluids, Vol 2; Wiley and Sons, 1954.

London, F.; Nature 141, 643, (1938).

Manchester, F.D.; Ph.D. thesis, University of British Columbia. 1955.

Mendoza, E.; Experimental Cryophysics, Chapt. 8. Butterworths, 1961.

Mercereau, J., Notarys, H. and Pellam, J.R.; see Toronto, (1961), p. 552.

Morse, P.M.; Vibration and Sound, 2nd ed. McGraw-Hill, 1948.

Mikhailov, N.N. and Govor, A.Ya.; Instrum Exper Tech (English*) 2, 402, (1962).

Osborne, D.V.; Nature 162, 213, (1948).

Osborne, D.V.; Phys Soc Proc A64, 114, 1951.

Pake, G.E.; Paramagnetic Resonance; Benjamin, Inc., 1962.

Pellam, J.R.; Phys Rev 75, 1183, (1949).

Pellam, J.R.; Progress in Low Temp. Phys., Vol 1, Chapter 3; North Holland Publishing Company, 1955.

Peshkov, V.P.; JETP 18, 867, (1948).

Peshkov, V.P.; JETP 19, 270, (1949).

Peshkov, V.P.; Sov Phys JETP (English*) 11, 580, (1960).

Pippard, A.B.; Elements of Classical Thermodynamics, Cambridge University Press, 1957.

Rayleigh; The Theory of Sound, Vol 2. MacMillan and Co., 1896.

Schuster, N.A.; Rev Sci Instr 22, 254, (1951).

Scott, H.H.; Proc I R E 26, 226, (1938).

Shepard, W.G.; Electronics, p. 200, Oct. 1953.

Snyder, H.A.; See Toronto (1961), p. 551.

Snyder, H.A.; Rev Sci Instr 33, 467, (1962).

---

* This refers to the English translation of the Russian journal.

Squire, C.F.; *Low Temperature Physics*, McGraw-Hill, 1953.

Strong, J.; *Procedures in Experimental Physics*, Prentice Hall,1938.

Terman, F.E. and Pettit, J.M.; *Electronic Measurements*, 2nd ed. McGraw-Hill, 1952.

Tisza, L.; *Jour de Phys et Radium 1*, 350, (1940).

Tisza, L.; *Phys Rev 72*, 838, (1947).

Toronto; Proceedings, *7th International Conference on Low Temperature Physics*, University of Toronto Press, 1961.

Ward, J.C. and Wilks, J.; *Phil Mag 42*, 314, (1951).

Wheatley, J.C., Griffing, D.F. and Estle, T.L.; *Rev Sci Instr 27*, 1070, (1956).

White, D., Gonzales, O.D. and Johnston, H.L.; *Phys Rev 89*, 593, (1953).

White, G.K.; *Experimental Techniques in Low Temperature Physics*, Oxford University Press, 1959.

Wood, A.B.; *A Textbook of Sound*, Bell and Sons, Ltd., 1930.

Zemansky, M.W.; *Heat and Thermodynamics*, 4th ed. McGraw-Hill, 1957.

Zinov'eva, K.N.; *Sov Phys JETP* (English*) *4*, 36, (1957).

---

* Refers to the English translation of the Russian journal.